Clemson University

TigerPrints

All Theses

Theses

12-2021

Visualizing Features From Deep Neural Networks Trained on Alzheimer's Disease and Few-Shot Learning Models for Alzheimer's Disease

John Reeder
jreeder@clemson.edu

Follow this and additional works at: https://tigerprints.clemson.edu/all_theses

Part of the Artificial Intelligence and Robotics Commons, Data Science Commons, and the Other Computer Sciences Commons

Recommended Citation

Reeder, John, "Visualizing Features From Deep Neural Networks Trained on Alzheimer's Disease and Few-Shot Learning Models for Alzheimer's Disease" (2021). *All Theses*. 3679.
https://tigerprints.clemson.edu/all_theses/3679

This Thesis is brought to you for free and open access by the Theses at TigerPrints. It has been accepted for inclusion in All Theses by an authorized administrator of TigerPrints. For more information, please contact kokeefe@clemson.edu.

VISUALIZING FEATURES FROM DEEP NEURAL NETWORKS TRAINED ON ALZHEIMER'S DISEASE AND FEW-SHOT LEARNING MODELS FOR ALZHEIMER'S DISEASE

A Thesis
Presented to
the Graduate School of
Clemson University

In Partial Fulfillment
of the Requirements for the Degree
Master of Science
Computer Science

---

by
John G. Reeder
December 2021

Accepted by:
Dr. Kai Liu, Committee Chair
Dr. Brian Dean
Dr. Nianyi Li

Abstract

Alzheimer's disease is an incurable neural disease, usually affecting the elderly. The afflicted suffer from cognitive impairments that get dramatically worse at each stage. Previous research on Alzheimer's disease analysis in terms of classification leveraged statistical models such as support vector machines. However, statistical models such as support vector machines train the from numerical data instead of medical images. Today, convolutional neural networks (CNN) are widely considered as the one which can achieve the state-of-the-art image classification performance. However, due to their black box nature, there can be reluctance amongst medical professionals for their use. On the other hand, medical images are not easy to get access to, in contrast to general image datasets, such as CIFAR-100, due to several reasons, including privacy and professional cost, motivating us to train the model with high accuracy based on few samples. This thesis focuses on two perspectives: the first interpreting what the CNN model has learned in each layer and will the learned features vary with different input; and second, how to train a reliable network with high accuracy on few medical imaging samples. To address the questions raised above, two different models are examined. First, we use a conventional residual CNN and experiment with two different training methods. The first uses a standard training schedule where the model's weights are initialized randomly and the second uses transfer learning where we use the weights of a model trained on a larger dataset of a different task as the initial weights for our model. Our method can yield the accuracies of 98.5% and 99.53%, respectively. Our second model studies metric learning instead of classification. In this method the model learns to group images that are similar. The model is fed with a very small set of samples per class, so-

called Few-Shot learning. The goal is to learn how similar an image is from another. The model can learn deep embedded representations of an input such that similar inputs are close together in the embedded space and dissimilar inputs are far apart.

Acknowledgments

First and foremost, I am extremely grateful to Dr. Kai Liu for all his guidance and support during my Masters program. I would also like to thank Dr. Brian Dean and Dr. Nianyi Li for being part of my committee. Many thanks to all my friends and relatives that encouraged me throughout my degree. Finally, I would like to thank my parents for all the love and support they provided over the years to get me to this moment.

Table of Contents

List of Tables

List of Figures

Chapter 1

Introduction

Alzheimer's disease is an incurable disease. It accounts for 60% to 80% of all dementia cases [1]. Early symptoms include memory loss, apathy, and depression. These get drastically worse as the disease progresses, causing impairment of communication, and disorientation, as well physical impairments such as inability to walk [1]. As of 2021, 5.3% of people between 65 and 74 are diagnosed with Alzheimer's disease [1]. This rate increases drastically the older the population; 13.8% for people 75 to 84 years old and 34.6% for 85 and older [1]. However, old age alone does not cause Alzheimer's disease: other factors such as genetics as well as family history play a part in developing Alzheimer's disease. Even though genetics and age are unchangeable risk factors, there are preventable risk factors that play a part in developing Alzheimer's disease later in life. Factors that can increase risk include smoking, diet, and lifestyle. Recently, it was discovered that Alzheimer's disease can begin long before any symptoms, 20 years or more in some cases [1].

Applying machine learning techniques to medical imaging has become a large area of interest. Being able to accurately identify different diseases automatically could cut down on misdiagnosis as well as detecting the initial onset of certain diseases. Alzheimer's disease is one of these. Previous research for Alzheimer's disease classification has shown success using statistical means such as support vector machines. However, these methods rely on training from numerical data rather than images. Today, deep learning models such as convolutional neural networks (CNN) are the models used to achieve state-of-the-art accuracy for image classification. They benefit from training directly on the dataset images. There are, however, some downsides to using CNNs. First, currently CNNs are a black-box approach. In some problem domains this is not a concern. However, in biomedical imaging there is a need for the method to be reliable and explainable given the sensitive nature of the data. Second, CNNs require large amounts of images in order to train a model that will generalize well. In medical imaging, gathering large amounts of imaging data is not easy due to several reasons, including privacy and professional cost. This thesis will address both of these problems. For the first problem, we focus on how to extract features from a conventional CNN trained on adequate amounts of data. We explore two different methods to train the model. For the first method we train the network from randomly initialized weights, and for the second, we train the model using weights transferred from another task. For the second problem, we use a technique called few-shot learning. In this method, we train the model with very few samples per class. We use two different metric learning models to accomplish this: the Siamese network and the triplet network.

1.1 Problem Statement

Detection of Alzheimer's disease is an important tool for radiologists and physicians. Previously, most research focused on using statistical methods to analyze medical data to construct classification models. More recently, research has focused on using deep learning models to accomplish this task. It has been shown numerous times that these models prove to be very accurate at correctly detecting different stages of Alzheimer's disease [8, 16, 21, 26, 27, 31]. However, there has been a scarce amount of research on feature explainability for Alzheimer's disease trained models. The research that has been done has used three dimensional CNNs [21, 27]. In this thesis, we use a similar visualization method as Oh et al. [21] and Rieke et al. [27], however, we use two dimensional CNNs similar to [8, 26, 31]. We will also explore a different technique for visualizing features first introduced by Mordvintsev et al. [18].

Medical imaging is often difficult to obtain due to numerous reasons. Traditional CNNs require large amounts of data which might not be obtainable given the constraint. In order to train a deep learning model with limited data we have to change how it learns. We focus on two metric learning models that have some prior use in medical imaging [4, 16, 17, 29]. This previous research has mainly used large datasets, however, we only train on a very limited amount.

1.2 Thesis Organization

This thesis consists of seven chapters. First, an introduction describing Alzheimer's disease and the research problem. Second, highlights of some important background information fundamental to the research problem. Third, expansion upon the previous chapter and examination of relevant previous research. The fourth and fifth, details of the work done and discussion. The sixth, discusses limitations and future work. The seventh, concludes the thesis.

Chapter 2

Background

In this chapter, four important topics are introduced before the main matter. First, is an overview of convolutional neural networks (CNN). Second, transfer learning is introduced and its typical application. Third, few-shot learning is introduced and typical models used. Finally, Feature Visualization is defined and described for its application in the thesis.

2.1 Convolutional Neural Networks

2.1.1 Vanilla Neural Network

In the most simplest example a vanilla neural network consists of three fully connected layers: the input layer, a so-called hidden layer, and an output layer. Figure 2.2 shows this simple model. The goal of this model is to learn a function, $F() : R^m \rightarrow R^o$, where m is the number of input dimensions and o is the number of output dimensions. The input layer takes in the input features, $X = [x_1, \ldots, x_n]$. These input features are then passed to the hidden layer where each node in the layer computes a linear weighted sum of all the nodes from the previous layer and its weights, see Figure 2.1. The weighted sum is then passed through a non-linear activation function and then finally to the output layer.

It is relatively simple to use this network to train on images. The 2d images are flattened into 1-d images and that is used as the input into the network. For simple vision

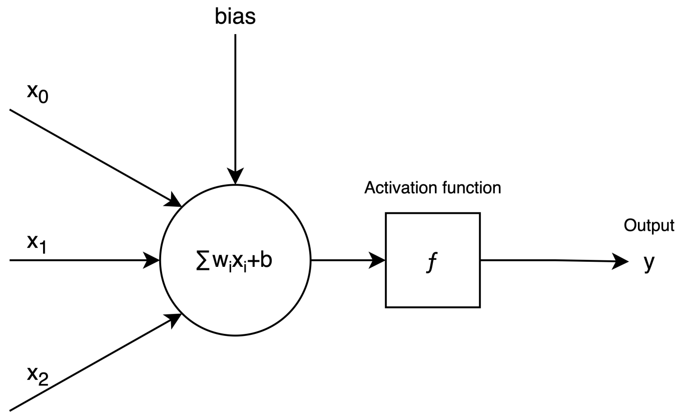

Figure 2.1: Individual Neuron

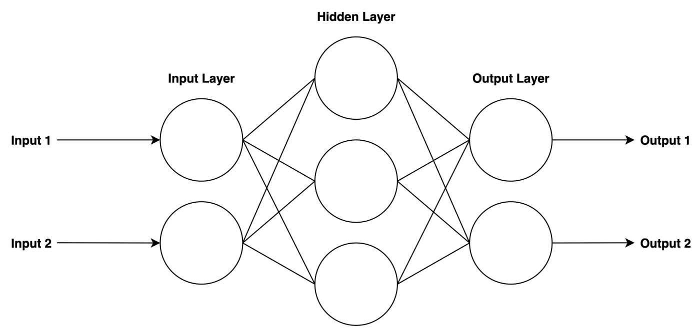

Figure 2.2: Vanilla Neural Network

tasks vannila neural networks work very well. However, for more complex tasks they do not. First, the amount of parameters required increases dramatically based on the size of the input image and how many hidden layers are used. If the image size is 100x100 then the first hidden layer requires 10,000 weights per neuron. Secondly, they do not account for spatial information in the images.

2.1.2 Convolutional Neural Network

A convolutional neural network is a type of artificial neural network. It is used mainly to solve computer vision problems. They were originally developed as a way to mimic the human brain's pattern recognition [7]. The network is made of multiple layers

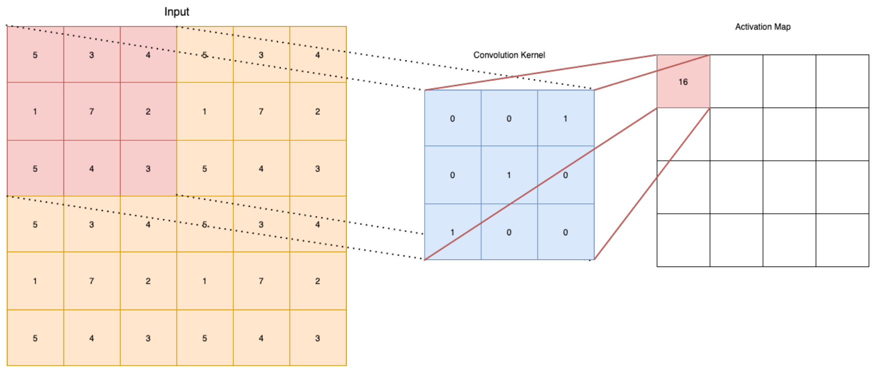

Figure 2.3: Convolutional Filter, an Example

of convolutions. Figure 2.3 shows an example of a convolution operation. The outputs from a convolution layer are called feature maps or activation maps. The output of each convolutional layer is passed to the next convolution layer until the final layer. Typically, the final layer flattens the feature map into a 1-d array and passes it through a fully connected layer with n-outputs, where n is the number of classes. Initially, the weights of the filters are started from random. Through the course of training, the filters are updated such that they extract the best features needed to solve the task, typically classification.

For computer vision tasks these outperform vanilla neural networks in two ways. First, the convolutions account for spatial information in the input. Second, a convolutional layer requires far fewer trainable parameters compared to the vanilla neural network. For these reasons they are typically used over vanilla neural networks for computer vision tasks.

2.2 Transfer Learning

Transfer learning can be defined as: using knowledge learned on one task, use it as the basis for solving a new task. This is possible due to how CNNs typically learn. The first layers typically have features that resemble Gabor filters or color blobs [32]. These features then turn into simple patterns. At the very last layers, features are very specific to the task. By taking advantage of the fact that most CNNs learn in this fashion, most or all layers can be reused for the starting point for another task. This is beneficial if we have a dataset with limited amount of samples. With a limited amount of samples it might be impossible for the network to learn without overfitting. By transferring the weights of the network trained on a very large dataset we can reuse them on the new task. Depending on the size of the network, the transferred features are either fine-tuned or frozen. Yosinski et al. [32] described that fine-tuning may cause overfitting if the size of the network is large and the dataset very small, so it is best to “freeze” the layers. They also found that if the network is small, then the transferred layers could be fine-tuned for better performance [32].

The most common dataset used as the source is the ImageNet dataset [5]. The dataset contains 1000 classes of varying sources. Classes range from natural, such as animals and plants, to man-made, such as cars and boats. Since the range of classes varies drastically, for most applications it provides better results than if having trained from randomly initialized weights.

2.3 Few-Shot Learning

Deep learning models require large amounts of data to learn without overfitting. In contrast, the human brain is capable of remembering new objects having only seen them a few times prior. This is the goal that few-shot learning is trying to achieve. There are many different lines of research devoted to this task, but this thesis focuses on the metric learning method. In metric learning the goal is to learn embedding function that causes the embedding distance between similar classes to be small and dissimilar classes to be large. There are numerous models that can be used for this type of learning but two popular ones are: Siamese Network and Triplet Network. A Siamese network trains a pair of neural networks that share weights. A Triplet network trains on a trio of neural networks that share weights. These models will be further discussed in Chapter 5.

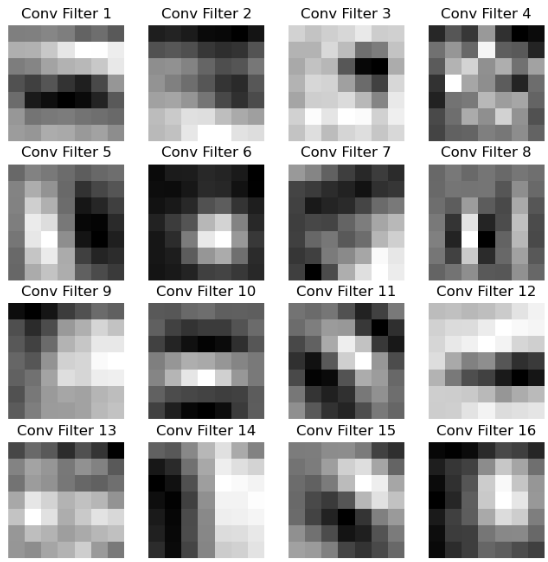

Figure 2.4: Convolution Filters Visualization

2.4 Feature Visualization and Attribution

As the name implies, feature visualization deals with visualizing the features a neural network has learned. Similar to feature visualization, attribution deals with figuring out what parts of the input triggered the highest response in the network. Both of these techniques are important for helping to explain and interpret neural network models. Figure 2.5 shows an example extracted feature from ResNet-18 trained on the ImageNet dataset. Figure 2.4 shows the filter weights for the first sixteen layers of the first convolutional layer of ResNet-18 trained on ImageNet.

2.5 Summary

In summary, vanilla neural networks are unable to perform well on more complex vision tasks. Their counterpart, a CNN, however, does and has become the typical neural model used for imaging tasks. Secondly, transfer learning is an important technique used

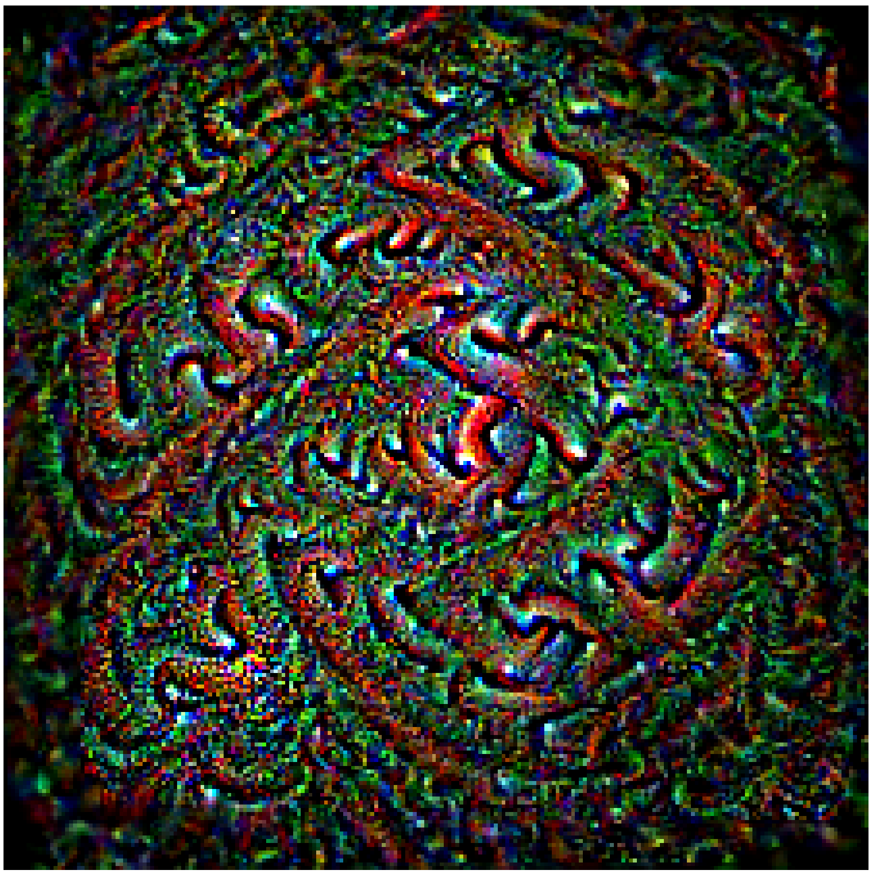

Figure 2.5: Positive Feature Extraction, an Example

to jump start a model to learn a new task. This could be for a few reasons: the smaller target dataset is closely related to the larger original dataset, or the target dataset could have fewer samples. Third, few-shot learning is a technique used to mimic how the human brain can recognize objects having only seen them a handful of times before. One method used is metric learning, where a model transforms the models into an embedding space and increases the distance between dissimilar objects and decreases the distance between similar ones. Finally, feature visualization and attribution are techniques used to help explain or interpret what deep learning models are learning and recognizing.

Chapter 3

Related Work

In the last chapter, we introduced some of the important topics relevant to the research topic. In this chapter we examine more in depth specific applications and prior research on these topics. In this examination, four different areas of prior research will be discussed. First, we discuss transfer learning in the medical imaging domain. Second, we look at prior research dealing with classification of Alzheimer's disease. Third, we examine two few-shot learning models. Finally, we look at research on visualization techniques.

3.1 Transfer Learning in Medical Imaging Domain

Transfer learning has become a common method used in deep learning on medical imaging. Deep neural networks require large amounts of data in order to generalize well; large amounts of data for certain diseases can be hard to obtain. This is for a variety of reasons, such as: rare occurrence of certain diseases, or unable to obtain patient consent for use. The most common method used is to use a model trained on the ImageNet dataset and fine-tune it to the new dataset. Even though this method has been widely adopted, it is still not clear how it effects training on medical datasets such as MRI scans. Raghu et al. [25] studied the effects of transfer learning from the natural image domain to medical imaging. In their experiments they found that for a model that was trained from scratch did not have first layer convolution filters that resembled typical Gabor filters. When they trained the same model but with transfer learning, they found that there was minimal change in the first layer's convolution filters. They further explored and found that only the first few layers contribute to any meaningful feature reuse. Similar to them, we further explore how transfer learning effects the model's knowledge learned.

3.2 Alzheimer's Disease and Machine Learning

3.2.1 Statistical Methods

One of the most common statistical modeling methods used in prior Alzheimer's disease (AD) classification research is the Support Vector Machine (SVM). The goal of a SVM is two find a maximum margin hyperplane that separates two (or more) classes of data. In 2010, Salas-Gonzalez et al [28] proposed a SVM approach for single photon emission computed tomography (SPECT) scans for classifying if AD was present or not. In their method they select features using Welch's t-test, which is a t-test where equal population variances are not assumed. They perform Welch's t-test on each voxel for every sample and keep those which are greater than a threshold. They use these as the feature vector for input into a SVM with a linear kernel. Using their method they were able to obtain an accuracy of 95% with 10-fold cross validation using 79 samples. In 2013, Lahmiri and Boukadoum [14] proposed a different method for using SVMs on magnetic resonance imaging (MRI) scans. They extracted features from the imagery using multiscale fractal analysis to approximate Hurst's exponents. Hurst's exponents describe the long-memory dependence or persistence in a time-series signal. Using a polynomial kernel of degree 2 they achieved a classification of 99.18% with 10-fold cross validation on 93 samples. A year later, they extended their method to classify mild cognitive impairment (MCI) from AD, AD from normal, and a multiclass SVM for the three [15]. Their method produces high accuracies of 97% for MCI vs healthy, 97.5% for MCI vs AD, and 94% for multi-class on 33 samples with 10-fold cross validation.

More recently, Altaf et al. [2] proposed a different method for using SVM. The model trains on features from not only the images but also clinical information. They use three different questionnaires ranging from questions about daily chores, to emotional well-being. They experimented with different texture based feature extraction methods such as: gray-level co-occurrence matrix (GLCM), scale invariant feature transform, local binary pattern, histogram of gradients, and bag of words. They found that GLCM features in addition to clinical features provided the best performance with 98.4% accuracy on binary classification, i.e. AD or Normal, and 79.8% accuracy on multi-class classification.

There are a few key observations to make from these past works. First, they test their methods with very small datasets. In the case of Lahmiri and Boukadoum [15], the total size of the dataset was 33 samples, and because they use 10-fold cross validation only 3 of these are used for testing. Secondly, none of the methods use raw image data to train the model. All of them rely on other preprocessing and feature extraction methods using other statistical methods.

3.2.2 Deep Learning Methods

In contrast to statistical methods like SVM, deep learning, in general, use models that learn to extract the features themselves. This allows the model to learn novel features that are not extracted via statistical methods. Recently, Alzheimer's disease classification research has shifted to using deep learning approaches. For example, Fulton et al. [8] propose two different approaches for classification using deep learning. First, they use ResNet-50 trained on MRI imagery from the OASIS-1 series dataset. They use random transformations as a preprocessing step so the model can adapt to deviations that are possible in the data. They used random rotations, random zooming, random shifting and shearing, and random horizontal flipping. With this method they are able to achieve an accuracy of 98.99% on the validation set. For their second model they used a gradient boosted model that was trained on clinical information. They include statistics such as: age, mini-mental state exam (MMSE), eTIV (intracranial volume), nWBV (brain volume), and ASF (atlas scaling factor). They also include qualitative variables such as: gender, education, and socioeconomic status. Without the use of any imagery data their model was able to achieve 91.3% accuracy. They found that MMSE score and age were the two most important features for predicting the presence of Alzheimer's disease.

They are not the only ones to produce high accuracy results using a ResNet type model. Sun et al. [31] also use ResNet-50, but they exchange the ReLU activation function for the Mish activation function. The main problem with using ReLU is the dying ReLU. The ReLU function is expressed as $f(x) = max(x, 0)$. A dying ReLU is when a neuron output is always zero. There are numerous different activations to handle this such as Leaky ReLU, $f(x) = max(\alpha * x, x)$, where a small slope is used for negative values. Mish is a proposed alternative that restricts the negative range but has an unbounded positive range. Having a lower bound prevents overfitting and has strong regularization effects. Being unbounded above can prevent saturation which can slow down training. They also use a non-local attention layer between the fourth and fifth residual blocks. To transform the data they use a Spatial Transformer network that learns how to apply transformations. The accuracy for their method reached 97.1% on three different classes.

Even the smallest ResNet model can achieve very accurate results on Alzheimer's disease classification. Ramzan et al. [26] use ResNet-18 on fMRI data from ADNI. ADNI contains imaging from patients at six different stages of Alzheimer's dementia. They test three training methods for the model: from scratch, off the shelf transfer learning, and fine-tuned transfer learning. For both transfer learning techniques, they use a network pretrained on ImageNet. The "off the shelf" method refers to a type of transfer learning where the transferred weights are frozen and only the last layer, the classifier, are retrained for the new task. In the fine-tuning method the weights of more layers are fine-tuned to the task. In their research, they fine-tuned all layers. With minimal preprocessing to remove artifacts from the scans, they achieve accuracy of 97.37%, 97.92%, and 97.88% with the from scratch, off the shelf, and fine-tuned models, respectively.

All of these past works are missing one vital component: explainability. Each of the models is able to reach very high classification accuracies, but it is unclear what the models learned to achieve this. There has been previous research on explainability for Alzheimer's disease [6, 21, 27], however, it has been mostly done on models using 3-dimensional CNNs. In this thesis, we will use the same network architecture used in [8, 26, 31] and examine how to visually explain what the model has learned.

3.3 Few-Shot Learning Methods

Siamese neural networks were first introduced in the 1990s for signature verification [3]. They consist of two twin neural networks attached at the output layer. The goal is for the network to extract features from two inputs and compute the similarity between the two. Since then they have been adopted to the few-shot learning domain. Koch et al. [13] used them for character recognition for different alphabets. In their implementation, they use CNNs instead of only fully connected layers. Using CNNs gave them a few advantages over prior implementations: they are much better at extracting features from images, and they have fewer weights. Siamese networks use a contrastive loss [9], where the similarity between two embedded inputs is calculated by using a distance formula, typically euclidean or cosine similarity. The network then updates such that it pushes two samples further away if they are not the same class, or pulls them closer together if they are.

Hoffer et al. [11] proposed a similar but different model called the triplet network. In this network, there is a triplet of neural networks with shared weights. It takes as input three data points: an anchor, a positive, and a negative. The anchor and positive belong to the same class while the negative is from a different class. The model uses a triplet loss which maximizes the distance between different classes while minimizing the distance within a class. This has an added benefit over the contrastive loss of the Siamese network. Since we have information about how close a same class pair is and a differing class pair is we can update the model so the same class pair is pulled closer together while also pushing the differing class pair further away.

Currently Siamese and triplet networks are relatively unexplored in the few-shot medical imaging domain. Shorfuzzaman and Hossain [29] used a Siamese neural network for diagnosis of COVID-19 patients. They chose VGG-16 as the embedding model and which achieved an accuracy of 95.6% with only 10 samples per class. There has been some prior work with Siamese networks in a non few-shot learning setting as well. Chung and Weng [4] used Siamese CNNs to aid in the task of content based medical image retrieval (CBMIR). Content based medical image retrieval is used by clinicians to retrieve cases similar to theirs to aid in diagnosis [4]. Chung and Weng proposed that using a Siamese CNN can reduce the amount of detailed expert labeled data that was needed in prior work. Their results show that Siamese networks trained with minimal expert labeled data are just as effective as normal CNNs trained with exact expert labeled data. Liu et al. [16] use deep Siamese networks for detecting brain asymmetries associated with Alzheimer's disease and mild cognitive impairment. Their implementation differs from ours, in that they use features extracted using MRICloud, an automated segmentation pipeline while we use a CNN. They also use a large dataset to train, while we use just a few. In this thesis we present novel work using Siamese and Triplet networks for few-shot Alzheimer's disease classification.

3.4 Visualization Techniques

There are many different visualization techniques for deep learning models. First, there is the saliency map. A saliency map is an image that represents the spatial support for a class in an image [30]. In other words, it is an image that shows what regions in the input image contributed the most to the output of the model. This is one of the most widely used visualization techniques. Philbrick et al. [24] used saliency maps to verify a model trained to detect if a CT image was from the contrast enhancement phase. For research on Alzheimer's disease classification, these have been used to determine which region of the brain contributed most to detecting Alzheimer's disease [6, 21, 27]. However, it is important to note that the models they used were for 3-dimensional CNNs trained on volumetric data.

Another really common strategy to determine a model has learned is to visualize the weights of the convolutional layers, see Figure 2.3. These are helpful in seeing how transfer learning has worked, i.e. how much the pretrained filters have been altered [25]. One less common technique uses gradient descent to create an image that maximizes the activation in a certain layer. This technique was first used [30] as a "class appearance" model. Using gradient descent, they generate an image that maximizes a specific class score for a model. The result image is therefore what the model thinks represents a given class. Nguyen et al. [19] exploit this fact and show how networks can be fooled. Today, this method is known as "DeepDream" [18]. In their work, rather than only use the output layer as the optimization target, they apply it to any of the layers. In 2017, Olah et al. [22] expanded this work even further. They detailed different steps and precautions that needed to be done in order to produce compelling visualizations. In our work, we will focus on using saliency maps and the gradient descent method as they are more interpretable.

3.5 Summary

In summary, transfer learning in medical imaging is a commonly used method, however, it is unclear how it effects medical imaging tasks. Alzheimer's disease classification used to be done by statistical means. Most commonly, SVM were used and produced very high accuracies, however, they only validate on a limited amount of data. They also require hand selection of features to train on. A rapidly growing approach is to use deep learning on medical imaging. Deep learning models benefit by being able to learn novel features on their own, as well as train on large amounts of data. These have shown to produce high accuracies comparable to statistical methods, however, they are validated on a bigger set of data. The downside to deep learning methods is that they are a black-box model. In order to gain insight into what the models are learning, we can use different visualization techniques. Another problem with using deep learning is that it usually requires large amounts of data. Prior research in other domains has shown success in training models on small amounts of data, known as few-shot learning. Two metric models that are popular in other domains have shown success in medical imaging. However, currently, they are trained using large datasets.

Chapter 4

Deep Convolutional Neural Networks for Alzheimer's Disease Classification

In the previous chapter we examined the difference between statistical and deep learning methods. We saw that deep learning methods are able to learn to extract features from images on their own without the need to be "hand-picked" using other methods. However, this introduces a problem with being able to understand and interpret the model. In order to alleviate this problem we also examined different visualization techniques used for model explainability.

There are numerous different deep learning model architectures used for image classification. However, to focus on a model that has been used before for Alzheimer's disease classification, we focused on the ResNet architecture. Prior research has shown to be able to achieve high accuracies, $\approx 97+\%$, using this architecture for Alzheimer's disease classification [8, 26, 31]. One area they do not cover in their research is exploring what the model has learned. There has been research previously that explores what models trained on Alzheimer's disease have learned, but they have been focused on 3-dimensional data,

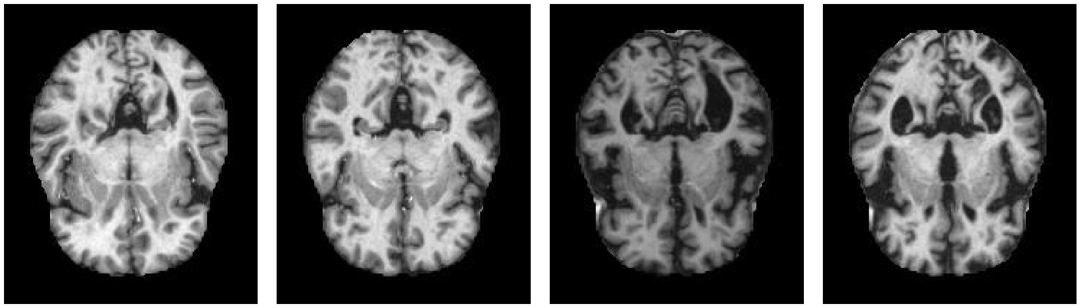

(a) Non-demented (b) Very Mild Demented (c) Mild Demented (d) Moderate Demented

Figure 4.1: Example images from dataset.

while ours is 2-dimensional.

In this chapter we examine how to create and train the model to achieve high accuracy. We use two different standard training techniques, random initialization and transfer learning. Then we detail how to extract the information learned by the model. Finally, we discuss how our methods can be used to examine the validity of the model.

4.1 The Dataset

To train our model, we used an open source Alzheimer's disease dataset obtained from Kaggle[1]. The dataset consists of 4 different stages of Alzheimer's disease: non-demented, very mild demented, mild demented, and moderate demented. Mild and moderate dementia stages are underrepresented in the dataset, with 896 and 64 samples for each, respectively. Non-demented and very mild demented stages have far more with 3200 and 2240 samples each, respectively. Each sample is a 176x208 grayscale image of a patient's brain on the axial plane taken with MRI. The location of the slice varies, however, there is no description of what ranges are used. There is also no indication of how many unique brains there are.

[1] https://www.kaggle.com/tourist55/alzheimers-dataset-4-class-of-images/version/1

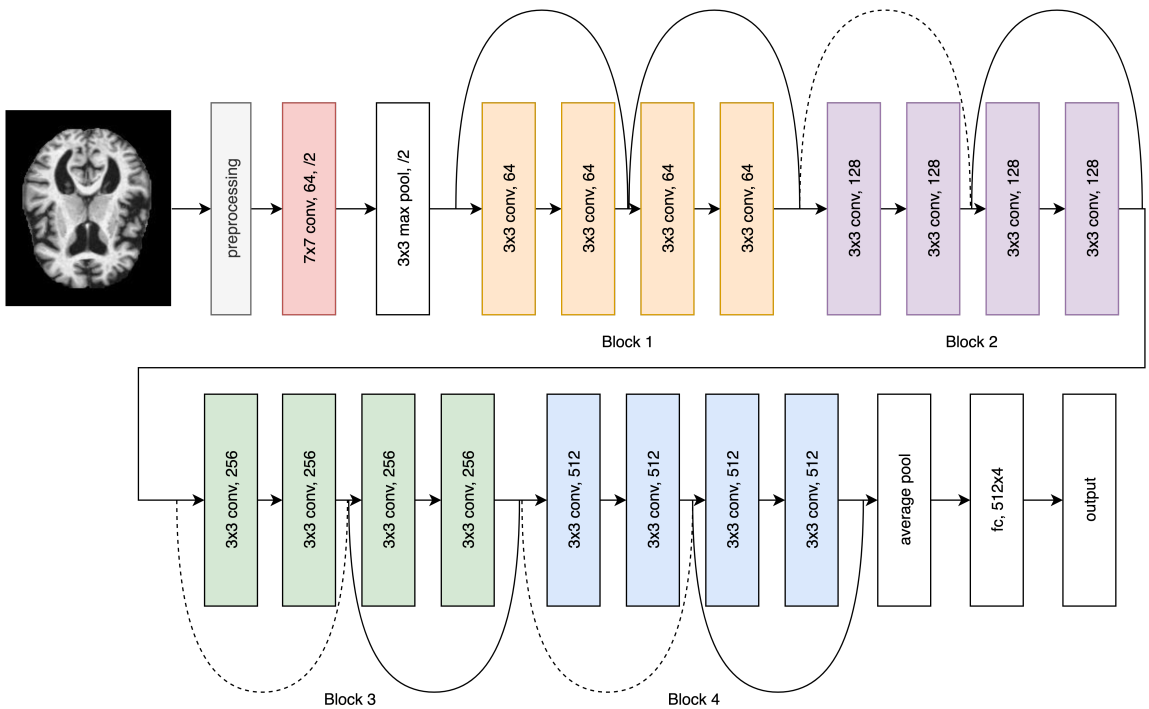

Figure 4.2: ResNet Model Architecture

4.1.1 Preprocessing

The dataset was split into an 80/20 train test split. Each class was shuffled and 80% of the samples were put in the training set, the rest were used as the test set. In order to prevent overfitting, we added some preprocessing transformations. First, the image is zero-padded to be 224x224 pixels in size which is required for the model. Next the images are randomly flipped left to right with $p = 0.5$. Next they are randomly rotated, we found $\theta = \pm 20°$ produces the best performance. These transformations help the model learn slight deviations in the input and are similar to those in prior works [8]. Finally, the images are normalized to have a mean of 0 and a standard deviation of 1, this serves to center the data for better training performance. Only normalization was applied to the test set.

4.2 The ResNet Model

Traditional deep convolutional neural networks suffer from a degradation problem. As the model becomes deeper, accuracy is saturated then rapidly degrades. He et al. [10] proposed that this could be overcome by using residual mappings. The mapping can be formally written as:

$$y = \mathcal{F}(x, \{W_i\}) + x$$

. The x and y indicate the input and output vectors and $\mathcal{F}(x, \{W_i\})$ is the residual mapping to be learned. This mapping can be implemented as a "shortcut connection", a direct connection that connects two non-consecutive layers in the model, and a simple element-wise addition. See Figure 4.2 for the full ResNet-18 model. The solid black connections indicate an identity shortcut, i.e. the same input and output shape, the dotted connection indicate an increase in size. The model takes as input the preprocessed grayscale image and passes it through an initial convolution and max pooling layer. It is then passed through 4 blocks of convolutional layers. Each of these blocks consists of 4 convolutional layers. After each convolution, batch normalization is applied followed by an ReLU activation function. The first convolution of blocks 2, 3, and 4 use a stride of 2 to downsample the feature maps. The output of the pooling layer is flattened into a 512 dimension tensor which is passed into the final output layer with four output units. During training time, we use a cross entropy loss to update the model's weights through backpropagation. For inference, the outputs are passed through a Softmax function which turns the outputs into probabilities between 0 and 1, and sum of 1.

4.3 Experimental Setup

4.3.1 The From Scratch Model

To implement our model we used a standard ResNet-18 model from the PyTorch deep learning framework [23]. To account for the single input channel of our dataset we

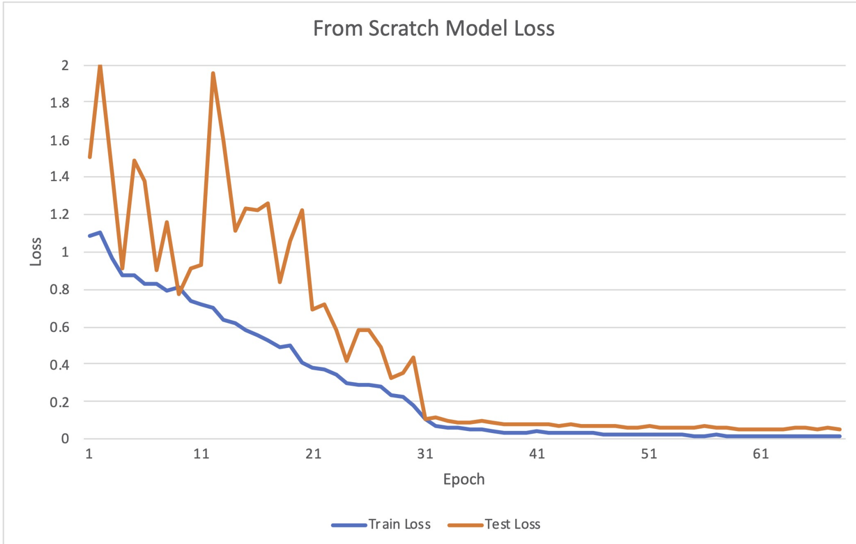

Figure 4.3: From Scratch Model Convergence

replace the first layer with an equivalent convolution layer except the input dimension was set as one, rather than three. Besides this change, no other modifications were necessary.

To train the model, we used stochastic gradient descent (SGD) optimization. We used an initial learning rate of $\alpha = 0.01$. This was decayed by $\gamma = 0.1$ after 30 epochs. A momentum factor of 0.9 was used, as well as L2 regularization with $\lambda = 0.00001$. Finally, we used a batch size of 128. All hyperparameters were chosen based on numerous trial runs; these provided the best results on the test set. After 68 epochs, the test loss converged. Figure 4.3 shows the training and testing losses. Figure 4.4 shows the test accuracy during training. The final recorded training and testing accuracy was 100% and 98.44%, respectively. Table 4.1 shows the confusion matrix for the trained model.

4.3.2 The Transfer Learned Model

The same ResNet-18 model from the PyTorch library was used for the transfer learned model. The model's weights were initialized from PyTorch's supplied ImageNet trained model. In the PyTorch implementation, their model has a top-1 accuracy of 69.758% and top-5 accuracy of 89.078% on ImageNet. For this model, we had to make two modifi-

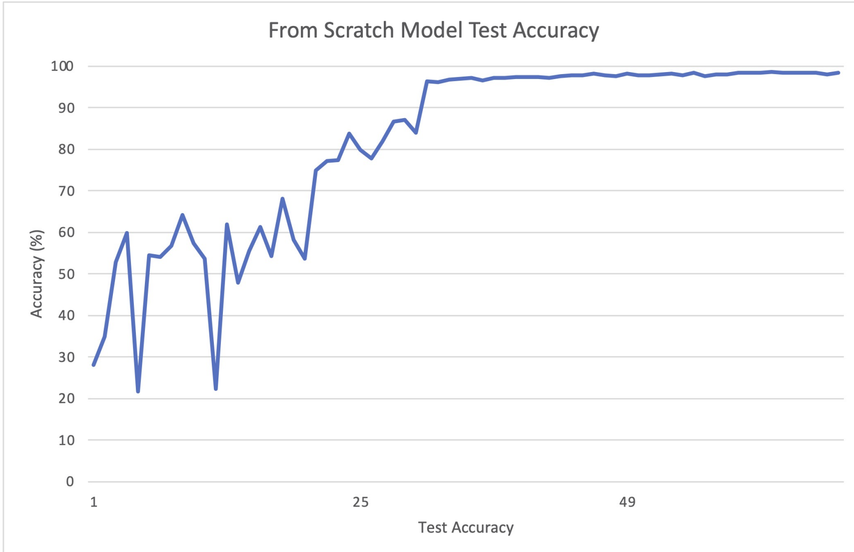

Figure 4.4: From Scratch Model Accuracy

cations. Similar to the "From Scratch" model, the first layer was replaced with an identical layer, but with one input channel. For the second change, we had to replace the final output layer. The original model was trained on one thousand different classes. The Alzheimer's dataset only has four, so the final output layer was replaced with one that has only four outputs. Besides these changes, no other modifications were necessary. All of the transferred layers were fine-tuned, which produced the best performance, in terms of accuracy.

Similar to the "From Scratch" model, SGD was used. We found that an initial learning rate of $\alpha = 0.01$ proved to be best. The learning rate decayed by a factor of 10 after 30 epochs. A momentum of 0.9 was used, as well as L2 regularization with $\lambda = 0.00001$. Finally, we used a batch size of 128. After 39 epochs, the test loss converged. Figure 4.5 shows the training and testing losses. Figure 4.6 shows the test accuracy. The final reported training and testing accuracy was 100% and 99.53%, respectively. Table 4.2 shows the confusion matrix for the trained model.

		Predicted			
		Non-Demented	Very Mild	Mild	Moderate
Actual	Non-Demented	630	8	2	0
	Very Mild	5	443	0	0
	Mild	2	2	175	0
	Moderate	0	0	0	13

Table 4.1: Confusion Matrix, "From Scratch" Model

		Predicted			
		Non-Demented	Very Mild	Mild	Moderate
Actual	Non-Demented	638	2	0	0
	Very Mild	0	448	0	0
	Mild	0	4	176	0
	Moderate	0	0	0	13

Table 4.2: Confusion Matrix, Transfer Learned Model

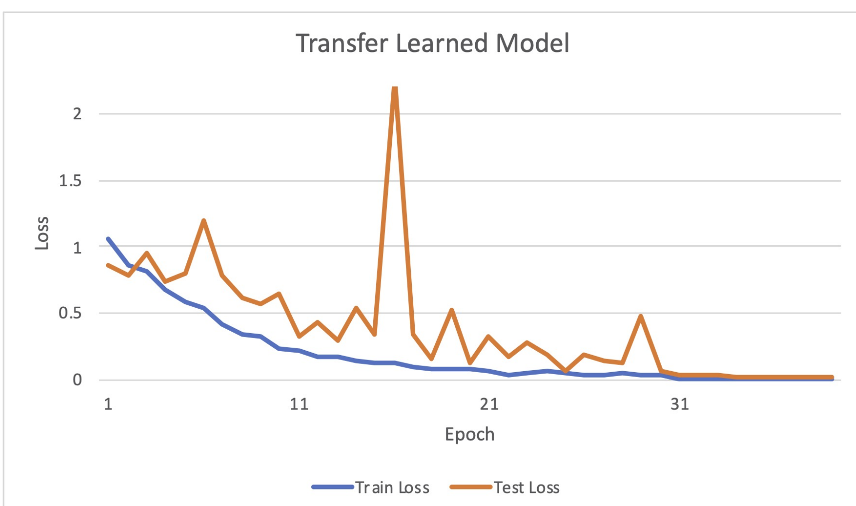

Figure 4.5: Transfer Learned Model Convergence

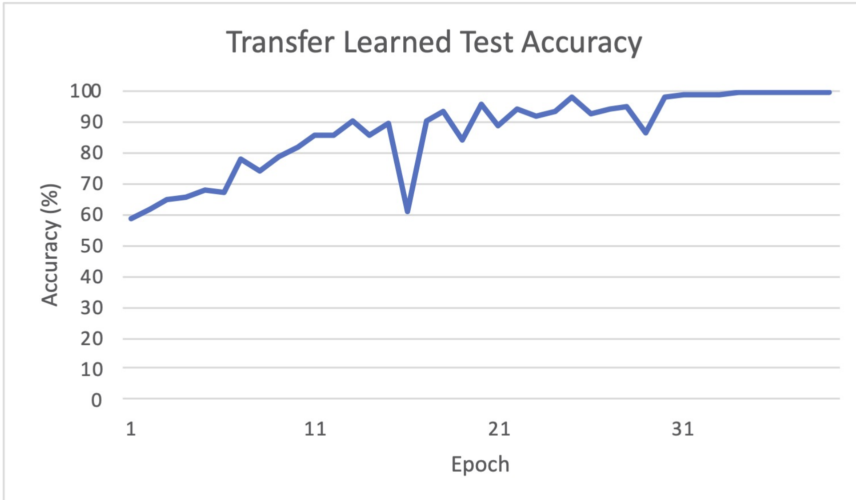

Figure 4.6: Transfer Learned Model Accuracy

4.4 Extracting the Features

To extract the features using optimization, we start with an image, feed it through our network and perform backpropagation on the image. The target goal is to either maximize or minimize the activation of a specific layer. Olah et al [22] found that different regularization techniques are required in order to obtain decent visualizations. Without regularization there tends to be too much noise and high-frequency patterns that are not comprehensible. Their article [22] detailed two different types of regularization: frequency penalization and transformations.

Frequency Penalization is used to reduce some of these high-frequency patterns. A Gaussian blur filter is used to reduce these patterns. They were originally used for creating fake images to fool a neural network into high-confidence predictions [19]. By definition, a Gaussian blur is a low-pass filter that eliminates high-frequencies. As a preprocessing step, a Gaussian blur is applied to the input prior to sending it through the model. A kernel size of 7 was selected and a random standard deviation was chosen between 0.1 and 2.0.

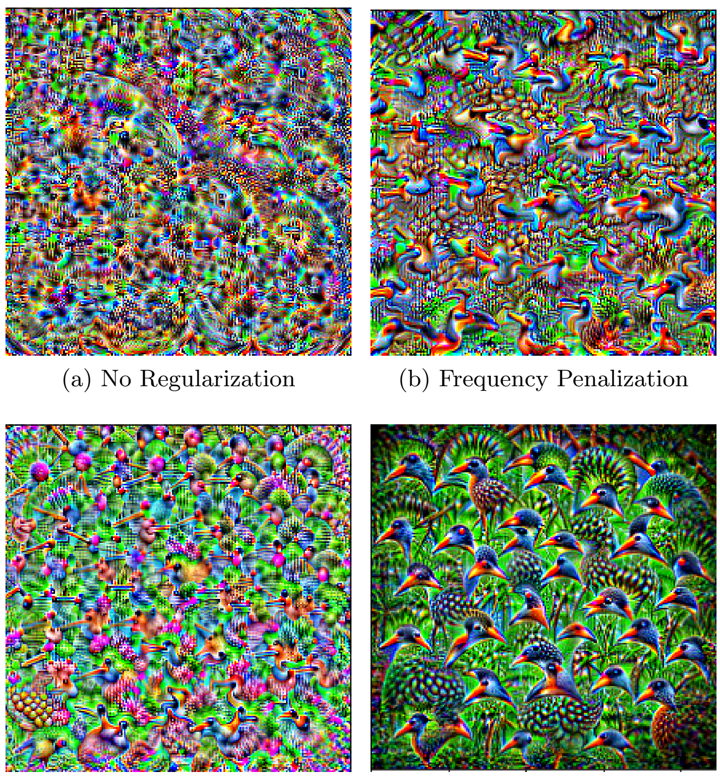

(a) No Regularization (b) Frequency Penalization

(c) Transformations (d) Frequency Penalization

Figure 4.7: Effect of Different Regularization

Transformations are also used to further reduce the noise in the output. Applying transformations randomly leads to extracting a feature that still responds highly even with small transformations. Three transformations were applied. First, the image is zero-padded on each side by 4 pixels, then it is randomly cropped then resized back to its original size. Finally, a random rotation of $\theta = \pm 15°$ is applied. Random cropping was first introduced for this task in 2015 by Mordvintsev et al. [18]. Using these simple transformations leads to better results.

Algorithm 1: Feature Extraction Algorithm

Input : Trained neural network Θ
Transformation function f
Target layer and channel θ_c
Output: Feature extracted $\mathbf{X} \in \mathbb{R}^{224\times224}$ s.t. $\Theta(\mathbf{X}) \rightarrow minimize(\theta_c)$

Randomly initialize $\mathbf{X} \in \mathbb{R}^{224\times224}$
for $i \leftarrow 0$ **to** T **do**
  Forward pass through network $\Theta(f(\mathbf{X}))$
  Calculate loss $\mathcal{L} = mean(\theta_c)$
  Calculate gradients of loss $\mathcal{L}$ with respect to $\mathbf{X}$. $\nabla = \frac{\delta\mathcal{L}}{\delta\mathbf{X}}$
  Update $\mathbf{X}$ via gradient descent. $\mathbf{X} = \mathbf{X} - \alpha * \nabla$
end

Figure 4.7 shows how each of these effects the feature we extract. The features were extracted from the same layer and channel all using the same hyperparameters. Without using any regularization it is clear to see the noise. By themselves, frequency penalization and transformations remove some of the noise, but most of it is still there. By combining them, we can obtain something that resembles something from our dataset. In this case, we can see what looks to be bird beaks and eyes.

4.4.1 Vanilla Extraction

To extract the features, the optimization technique was used. Adam was used as the optimizer for all feature extractions. Betas were left at default, $\beta_1 = 0.9$ and $\beta_2 = 0.999$. Epsilon was also left at default value, $\epsilon = 1 \times 10^{-8}$. AN L2 regularization of $\lambda = 0.0001$ was used. The starting image is initialized randomly from a normal distribution, $\mu = 0$ and

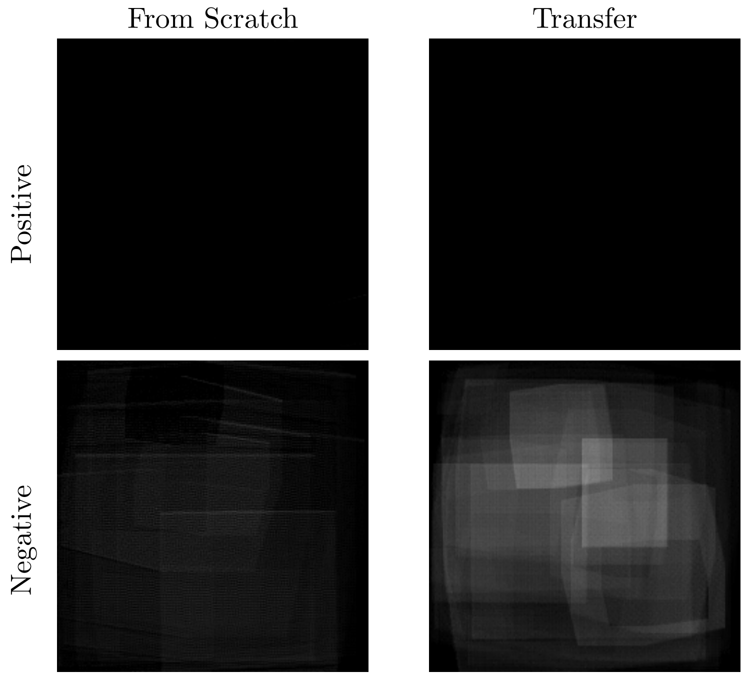

Figure 4.8: Features extracted from channel 0 from the first convolutional layer, "From Scratch" model

$\sigma^2 = 1$. The size was set to 224x224 pixels, as required for the model, and matches the training image size. This image is then passed through the transformation layer that applies the padding, random crop, random rotation, and random Gaussian blur. The transformed input is then passed through the previously trained model. On the forward pass, right after the input has passed through the target layer, the mean of the target channel is stored. This is used as the optimization target and used to perform backpropagation on the image. This process is done for 1000 iterations. See Figure 4.8 for the features extracted. It was a common occurrence for the starting layers to have a blank output. However, this does not mean that the channel or layer did not learn anything, just that the max activation for the channel was from a blank image. We will see in the next section that we can still obtain information about these channels. It is important to note that the original image is only updated via gradient descent, the transformations are applied as part of the model's pipeline.

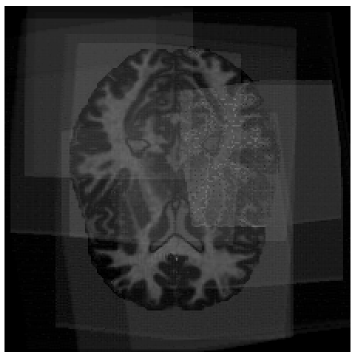

(a) Non-demented

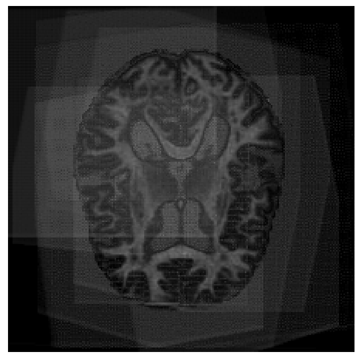

(b) Very Mildly Demented

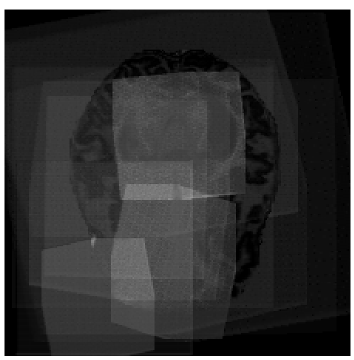

(c) Mildly Demented

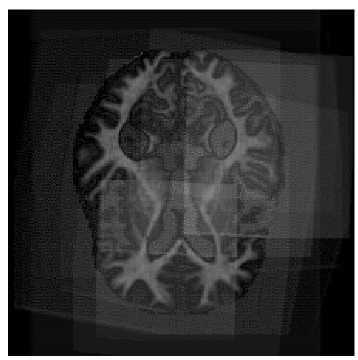

(d) Moderately Demented

Figure 4.9: Feature Extraction with Diversity, “From Scratch” model

4.4.2 Diversity Extraction

Due to the nature of optimization, the feature extracted may not be the only one that a specific layer "knows". We have also seen that it can also produce blank features. In order to see more of the features that might be encapsulated in a single layer, the starting input image is no longer initialized randomly. Instead, a dataset example can be used as the initial input. This process was first described by Nguyen et al. in 2016 [20]. The rest of the process remains the same; however, only 10 iterations are needed since we are only refining the image to achieve our optimization target. See Figure 4.9 for the visualization of these features that were extracted using diversity. In the figure, the features extracted were positive extractions from the same layer and channel as Figure 4.8, but started from a dataset image, each from a different class.

4.4.3 Saliency Maps

Another useful visualization tool is the saliency map. We can use saliency maps to visualize what areas our model responds highly to when it makes a prediction. These have been used in prior research to show that 3D CNN models are capable of recognizing areas typically affected by Alzheimer's disease [6, 21, 27]. These can be computed by passing an image through the model then calculating the gradient of the outputs with respect to the image. To see only the areas that affect the highest class prediction, we only calculate the gradient of the top predicted class. Figure 4.10 shows saliency maps for samples of each of the classes for the model trained from scratch. Figure 4.11 shows saliency maps for the same samples, but for the model trained using transfer learning.

Algorithm 2: Saliency Map Algorithm

Input : Trained neural network Θ
Query Image $\mathbf{I}$

Output: Saliency Map $\mathbf{X} \in \mathbb{R}^{224\times224}$

1 Forward pass through network $y = \Theta(\mathbf{I})$

2 Calculate gradient of $\arg\max(y)$ with respect to $\mathbf{I}$. $\nabla = \frac{\delta \arg\max(y)}{\delta \mathbf{I}}$

3 $\mathbf{X} = \|\nabla\|$

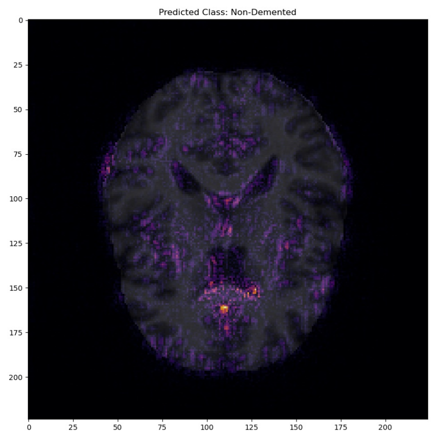

(a) Non-demented

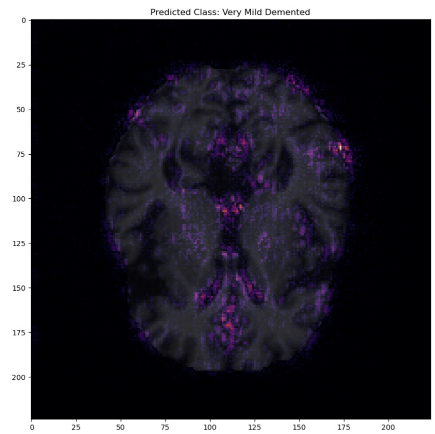

(b) Very Mildly Demented

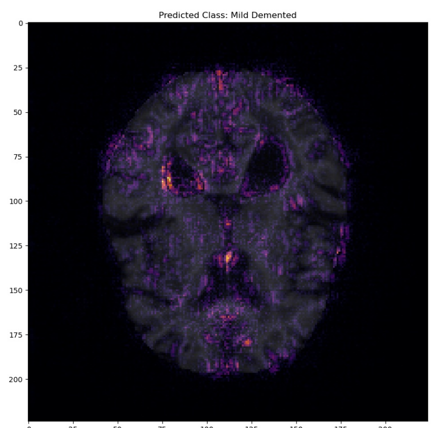

(c) Mildly Demented

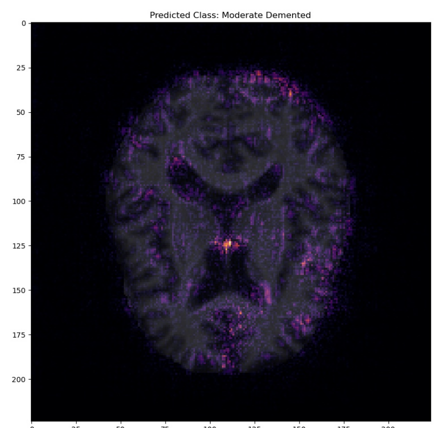

(d) Moderately Demented

Figure 4.10: Saliency Maps, “From Scratch” model

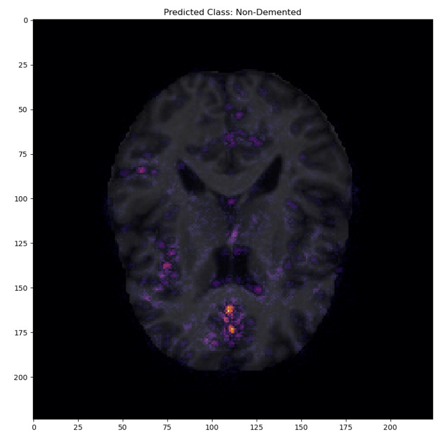

(a) Non-demented

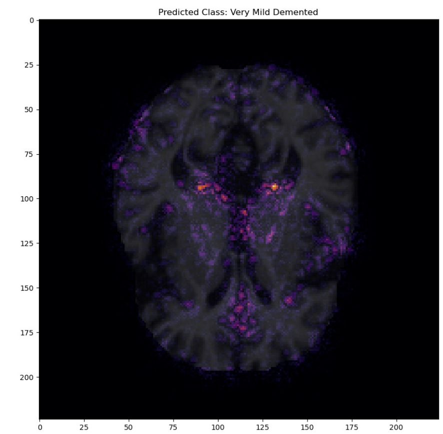

(b) Very Mildly Demented

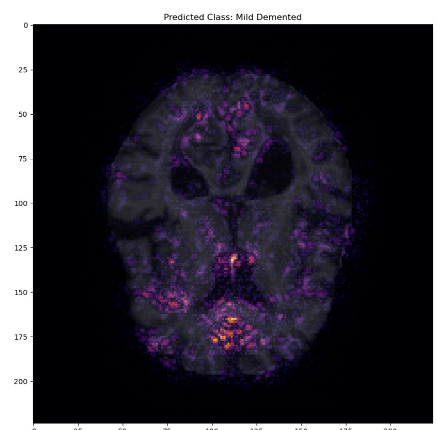

(c) Mildly Demented

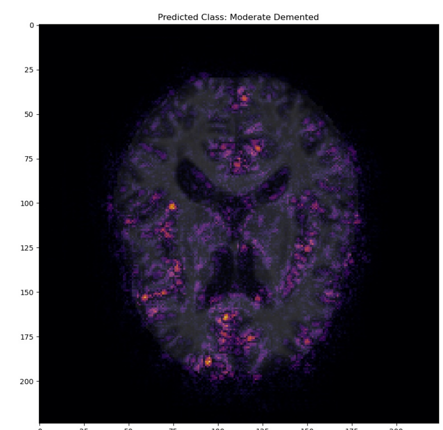

(d) Moderately Demented

Figure 4.11: Saliency Maps, Transferred model

4.5 Results and Discussion

Our "From Scratch" model performed very similar to the results in [8, 26, 31]. In one case, we achieved better [26], which is the same ResNet-18 model, however they use more classes. It is very close to the accuracy of [8] but our model uses fewer layers and thus much lighter weight. Our transfer learned model performed slightly better than the "From Scratch" model, $\approx 1\%$, with a test accuracy of 99.53%, which is higher than [8, 26, 31]; however, the purpose of this research is not to improve the classification accuracy.

Evaluating the features extracted from both of the models shows significant differences in learned features. Figure 4.12 shows the same channel and layer, but from different training method. The features are drastically different; indicating that the transfer learned model retains most of it's prior information. This is supported by the work done by Raghu et al. [25]. This effect is visible in all the other layers of the transfer learned model as well. Consistent with prior research, the "From Scratch" model's features become more complex deeper into the network. However, contrary to prior work [22, 18], the model does not learn complex features such as parts or objects. The deeper features in the model become complex edge and texture features. This might be due to the nature task. In ordinary datasets, classes can vary drastically, however, in this case most samples have very similar structure. On the other hand, the transfer learned model does still have parts and objects in the deeper layers. These are most likely remnants from being trained on ImageNet.

We can also see how the features change when given a different input. Figure 4.13 shows a feature extracted from the first channel and first convolution, but for different inputs. The top image in the figure is the feature extracted using the vanilla method, while the four images on the bottom use the diversity method. It appears that this layer segments out the white matter of the brain.

While the extracted features show what the model has learned, the saliency map shows what these learned features react to in a sample. Figure 4.10 and 4.11 show the saliency maps for the same inputs but for different training methods. It appears that both

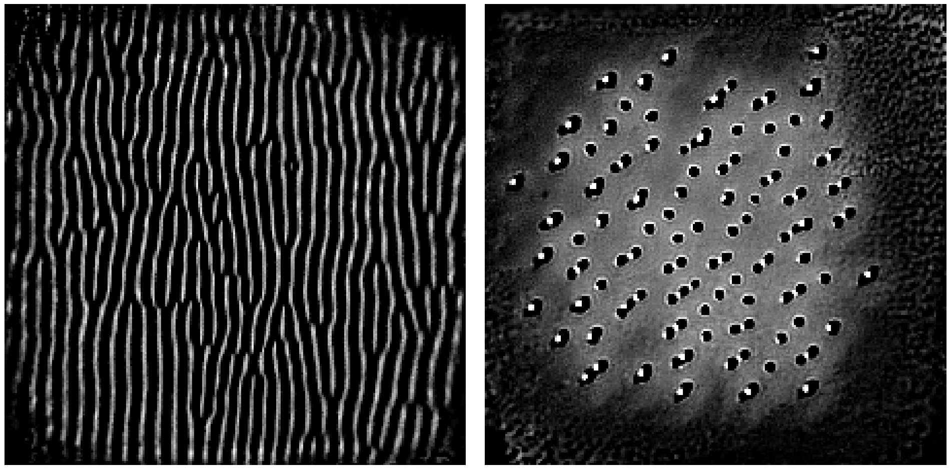

(a) "From Scratch" (b) Transfer Learned

Figure 4.12: Differences Between "From Scratch" and Transfer Learned, Positive Extraction

models react strongly to regions with gray matter. A study found that people suffering from Alzheimer's disease had reduced amounts of gray matter [12]. While the saliency maps do show that gray matter is important part in classification it does not explain why. However, gray matter is not the only reactive area; the ventricular regions have strong reactions in some areas. These results are similar to those found by Eitel and Ritter [6], however, they use 3-dimensional data and use binary classification. These findings should be validated with clinical professionals; the purpose of this work is to produce the visualizations.

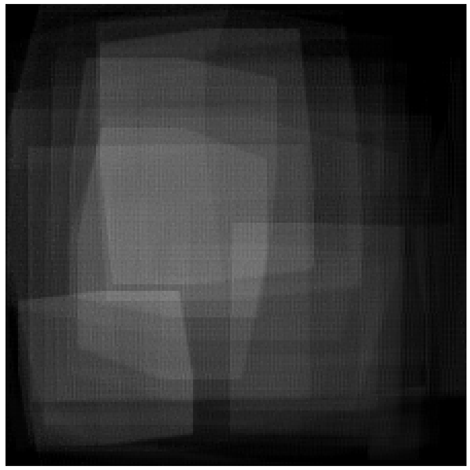

(a) Randomly Initialized

(b) Non-demented

(c) Very Mild

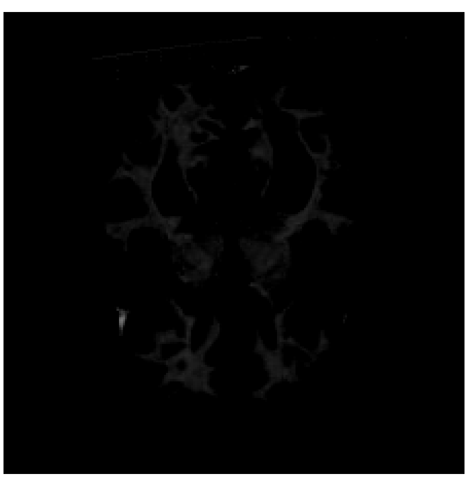

(d) Mild

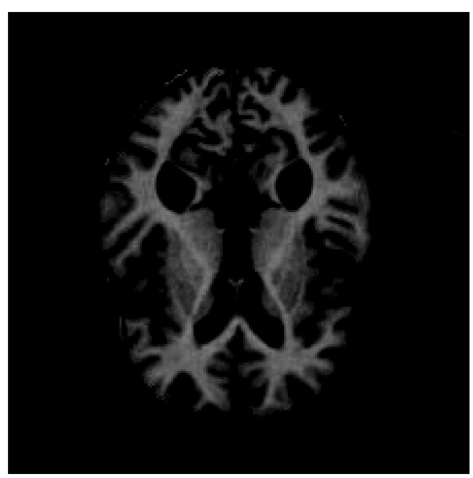

(e) Moderate

Figure 4.13: Feature Change, Negative Extraction

Chapter 5

Alzheimer's Disease and Few-Shot Learning

In the previous chapter, we address the problem of model explainability in medical imaging by training the model with adequate data. We showed that for two different learning methods, random initialization and transfer learning, both learn to react heavily to areas typically affected by Alzheimer's disease. In this chapter we address the second problem associated with deep learning: it requires large amounts of data. Previously, we examined two different models that can be used to reduce the amount data required to train accurate models. Namely, they are Siamese and Triplet networks. In previous works, these models were used mainly on large datasets. However, based on previous research, they are capable of learning with limited amounts of medical imaging data [29].

In this chapter, we examine how Siamese and Triplet networks can be used learn to classify Alzheimer's disease with limited data. We detail the ways we preprocess the data in order to train the model. To train both networks, we use similar methods as in the last chapter; we train the models both with random initialization and transfer learning. Finally, we detail how to use the trained Siamese and Triplet networks to classify, since their goal is not strictly classification.

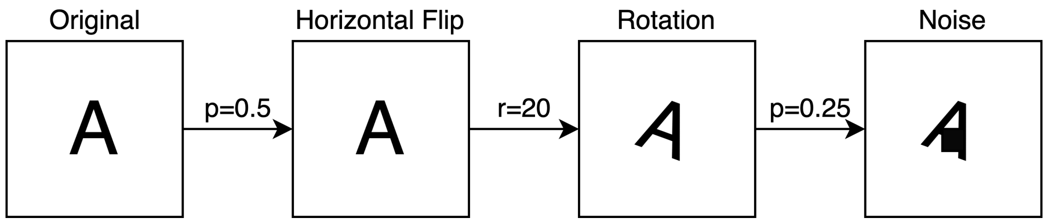

Figure 5.1: Transformation Pipeline

5.1 The Dataset

We use the same base dataset obtained from Kaggle as described in Section 4.1. For few-shot learning, we want to train the model only on a limited amount of data. We train with 25 random samples from each class. The rest of the dataset is used as the test set.

To prevent extreme overfitting, we apply random augmentations in an online fashion rather than offline. This helps to provide the network with constantly changing data. We apply random horizontal flipping with probability of $p = 0.5$ as well as a random rotation with $\theta = \pm 20°$. Finally, we inject noise into a random region with $p = 0.25$. We also normalize the images to have a mean of 0 and standard deviation of 1. The test set is only normalized. Figure 5.1 shows the entire transformation pipeline.

5.2 Siamese Network

A Siamese network is a pair of shared weight neural networks. It takes as input two samples, either two same class samples or samples from different classes. We use a contrastive loss function using euclidean distance:

$$\mathcal{L}(x, x^+) = y\|f(x) - f(x^+)\|^2 + (1 - y)(max(\alpha - \|f(x) - f(x^+)\|^2, 0))$$

Here, y denotes whether the classes are the same or different and α is the margin. With contrastive loss, the goal is to minimize the distance between a pair if the class is the same or maximize the distance between a pair with different classes, but only if the pair is within the margin.

5.3 Triplet Network

The Triplet network can be viewed as an extension of the Siamese net. Rather than two neural networks with shared weights, the Triplet network uses three. During the training phase we now pass three samples at a time, (x, x^+, x^-). Where x is a training sample, x^+ is a different sample from the same class, and x^- is a sample from a different class. The loss function is also changed to Triplet loss,

$$\mathcal{L}(x, x^+, x^-) = \max(\|f(x) - f(x^+)\|^2 - \|f(x) - f(x^-)\|^2 + \alpha, 0)$$

The goal is to minimize the L_2 distance between embeddings from the same class while maximizing the distance between different classes. Using both a positive and negative sample has the benefit of being able to both move same classes closer while moving different classes further away.

5.4 Embedding Network

To learn the feature embeddings we use a ResNet-18 CNN because we found it performs well at classification of Alzheimer's disease. Since we no longer classify, we remove the final output layer from the model. After the average pooling layer, we flatten the result and send it through a fully connected layer with n outputs, where n is our embedding dimension size. For our experiments, we use $n = 512$ as it performed best. See Figure 5.2 for the full model architecture. We test both a model with randomly initialized weights as well as a model transfer learned from ImageNet.

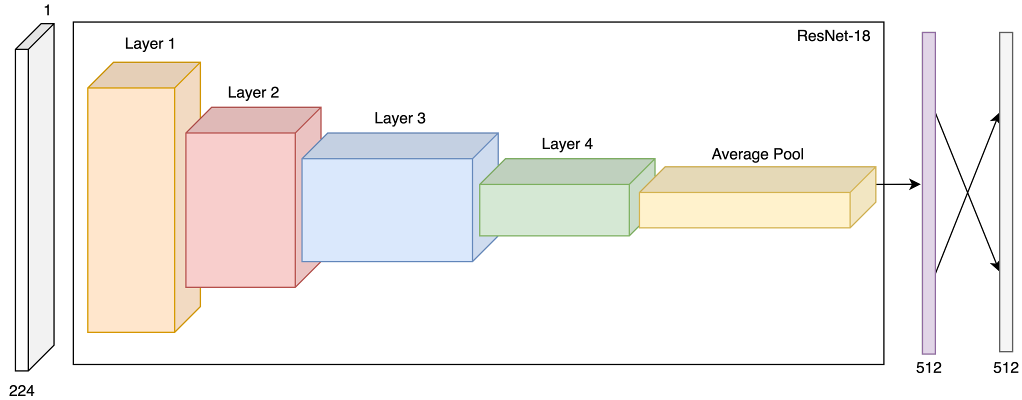

Figure 5.2: Embedding network used for Siamese and Triplet networks.

5.5 Experimental Setup

5.5.1 Siamese Network

To implement our models, we used the ResNet-18 model implemented in the PyTorch framework. The transferred learned model was initialized from the PyTorch framework ImageNet weights. We modified the network by removing the fully connected layer and replacing it with a fully connected layer each with 512 inputs/outputs. Training the Siamese networks was done using stochastic gradient descent (SGD). Both models used a starting learning rate of 0.1 and was decreased by a factor of 10 every 30 epochs. A momentum of 0.9 was used as well as L_2 regularization with $\lambda = 0.00001$. A batch size of 128 samples was used and the contrastive loss was computed for each possible pair. We chose a margin of $\alpha = 1.0$ through experimentation.

After training the model, we could visualize the embeddings by reducing them to two and three dimensions via PCA. Figures 5.3 and 5.4 show the embeddings reduced to two principle components for the "from scratch" and transfer learned models, respectively. Figures 5.5 and 5.6 show the embeddings reduced to three principles components for the "from scratch" and transfer learned model, respectively. To perform classification, we chose the closest embedding from the training set to each test sample embedding, i.e. k-nearest neighbor with $k = 1$, a method similar to what has been done in prior work [11]. It is important to note that k-nearest neighbor was performed in the full 512-dimensional space, not the two or three dimensional space obtained via PCA. This produced class averaged accuracies of 59.91% and 65.4% for “from scratch” and transfer learned Siamese models, respectively.

5.5.2 Triplet Network

The same modified ResNet-18 model used for the Siamese network was used for the Triplet network. Training the Triplet models was done using SGD. Both models used a starting learning rate of 0.01 and decreased by a factor of 10 every 30 epochs. A momentum of 0.9 was used as well as L_2 regularization with $\lambda = 0.00001$. A random batch of 128 triplets was chosen each iteration. We chose a margin of $\alpha = 3.0$ through experimentation. For the “from scratch” model, training time took 200 epochs before convergence. For the transfer learned model, training time took 100 epochs before convergence.

We can use the same process as with the Siamese network to visualize and classify the embeddings. Figures 5.7 and 5.8 show the embeddings reduced to two principle components for the “from scratch” and transfer learned model, respectively. Figures 5.9 and 5.10 show the embeddings reduced to three principle components for the “from scratch” and transfer learned models, respectively. To perform classification, we chose the closest embedding from the training set to each test sample embedding, i.e. k-nearest neighbor with $k = 1$. This produced class averaged accuracies of 59.1% and 64.4% for “from scratch” and transfer learned Triplet models, respectively.

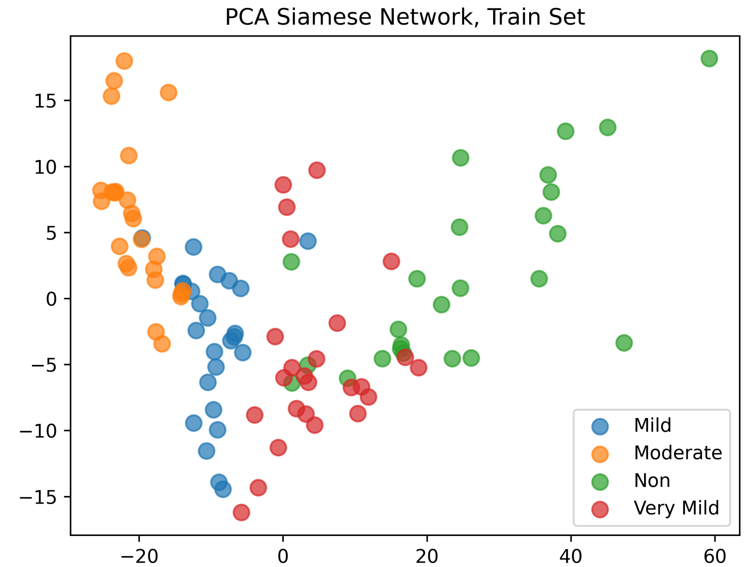

(a)

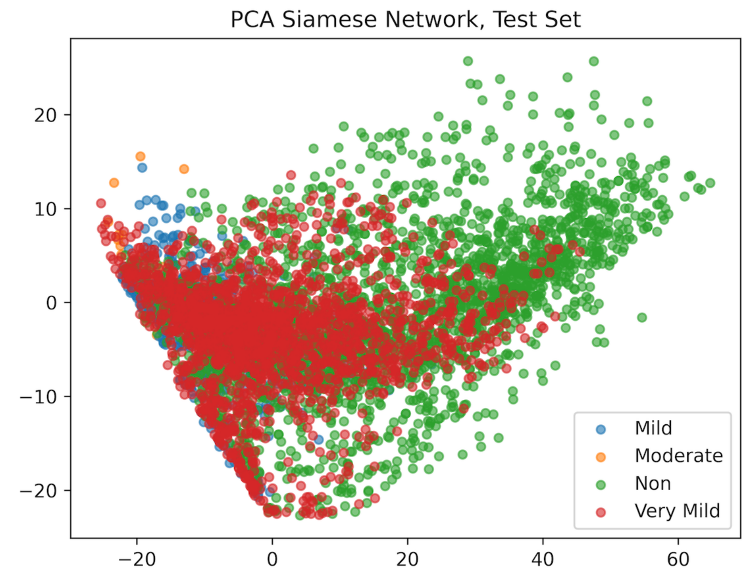

(b)

Figure 5.3: Siamese Network Embeds, “From Scratch” Model, 2-dimensions

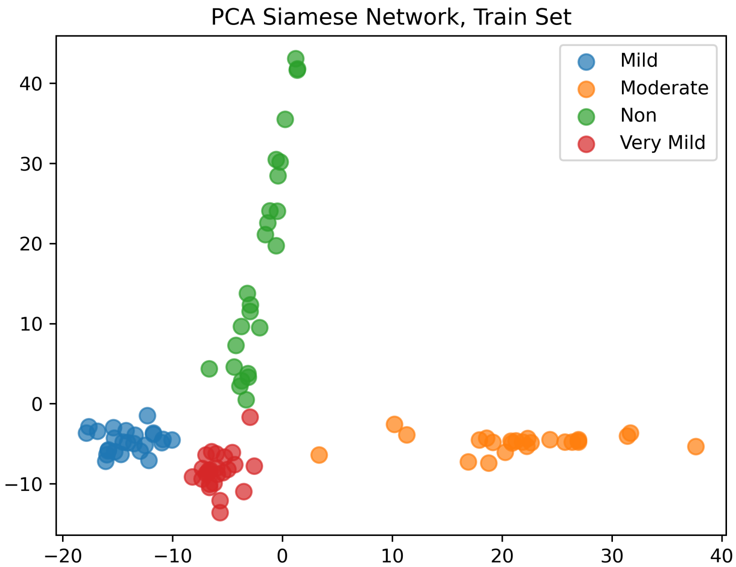

(a)

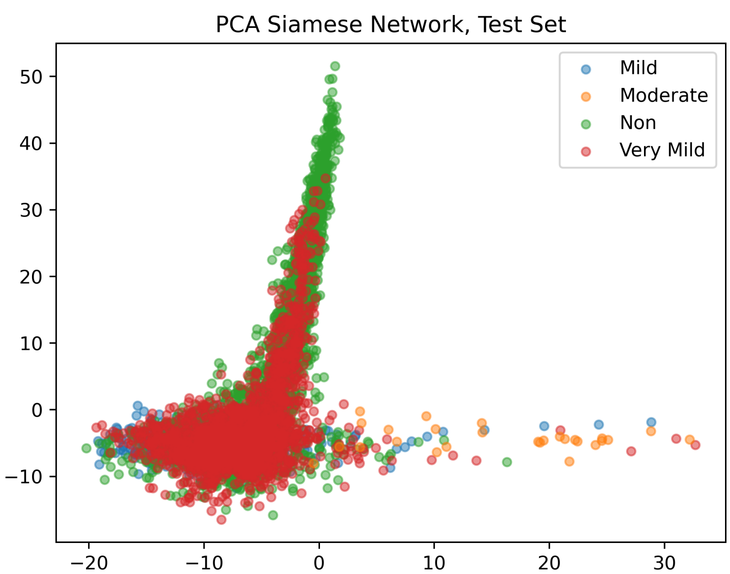

(b)

Figure 5.4: Siamese Network Embeds, Transfer Model, 2-dimensions

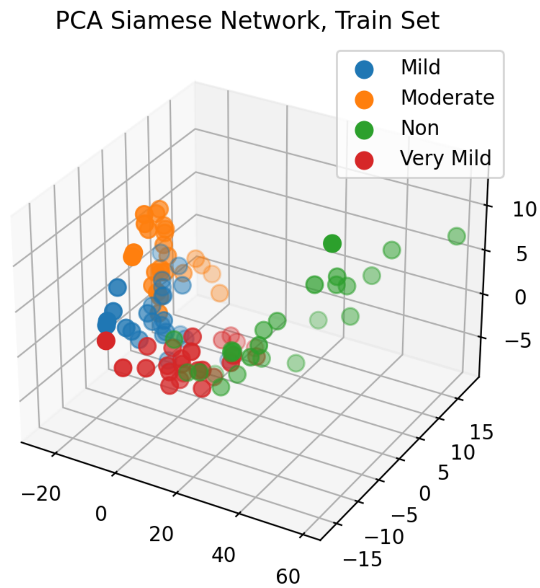

(a)

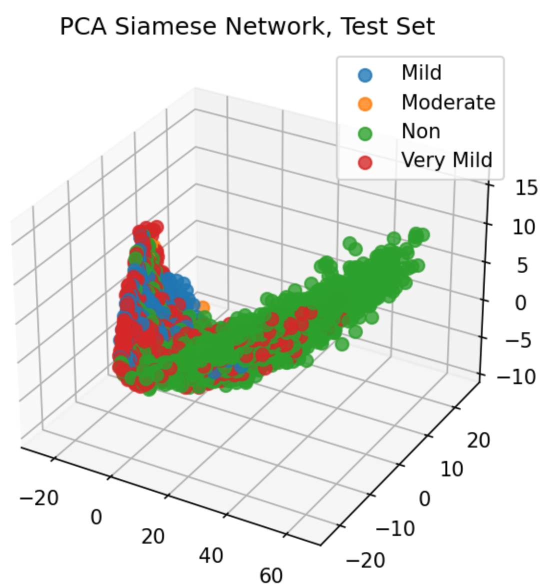

(b)

Figure 5.5: Siamese Network Embeds, "From Scratch" Model, 3-dimensions

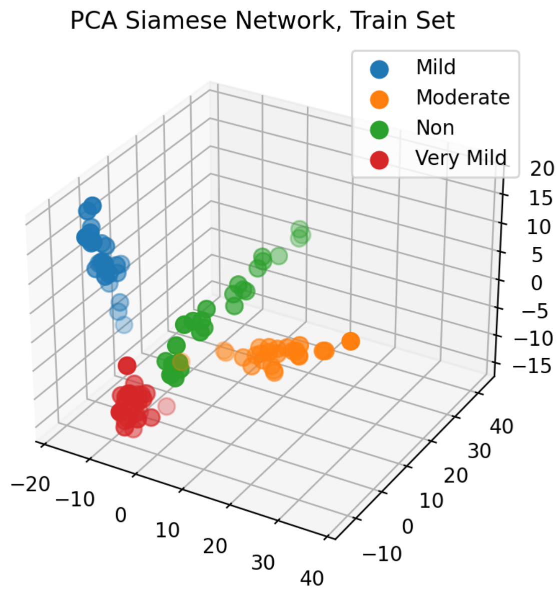

(a)

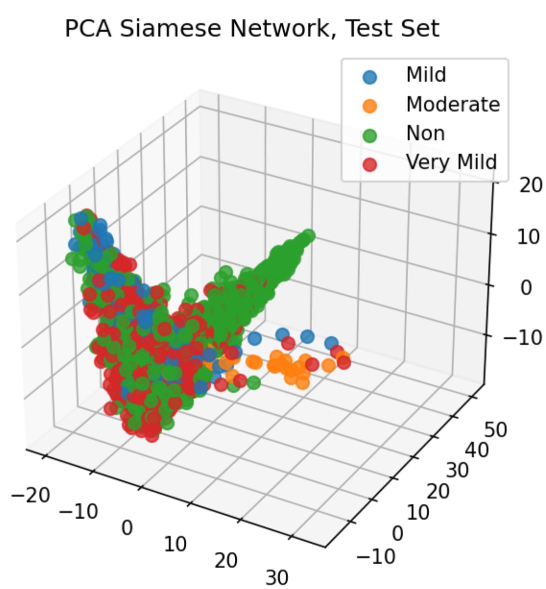

(b)

Figure 5.6: Siamese Network Embeds, Transfer Model, 3-dimensions

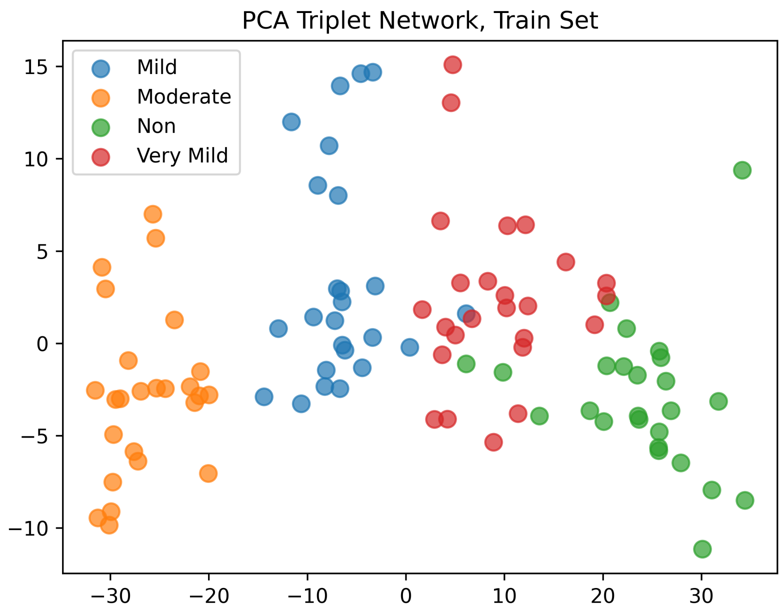

(a)

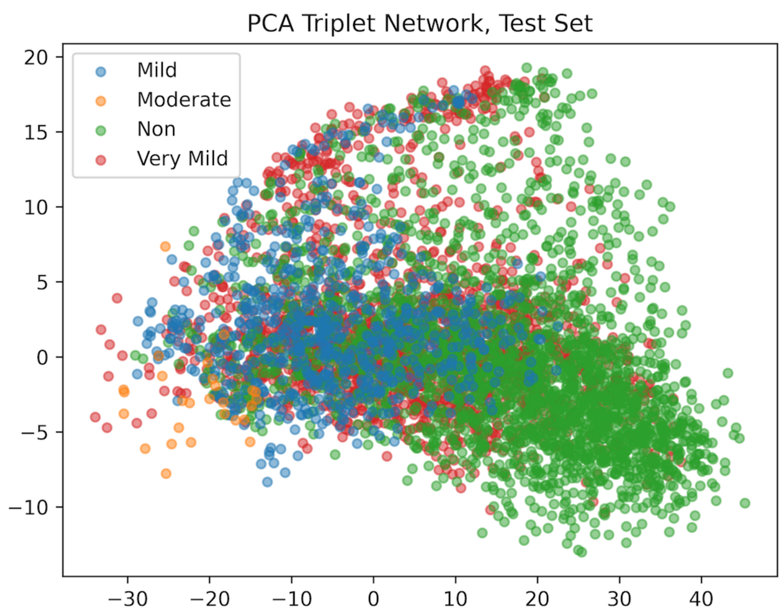

(b)

Figure 5.7: Triplet Network Embeds, "From Scratch" Model, 2-dimensions

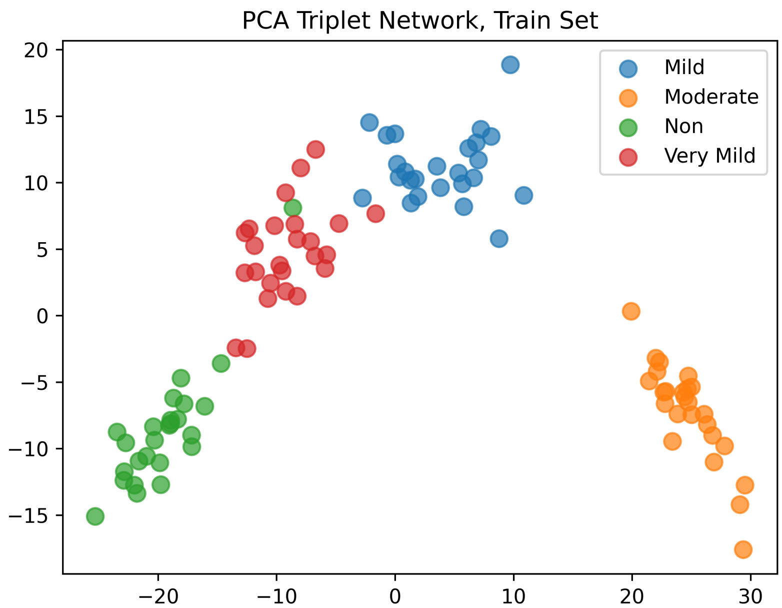

(a)

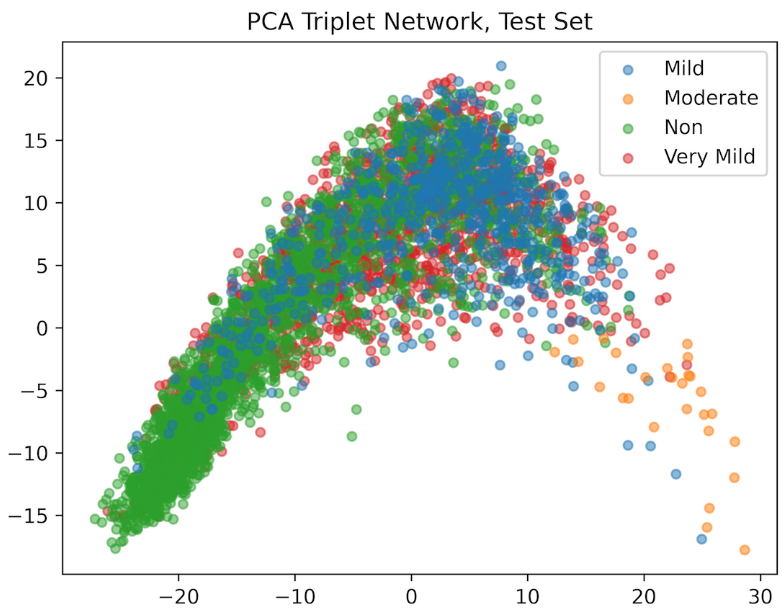

(b)

Figure 5.8: Triplet Network Embeds, Transfer Model, 2-dimensions

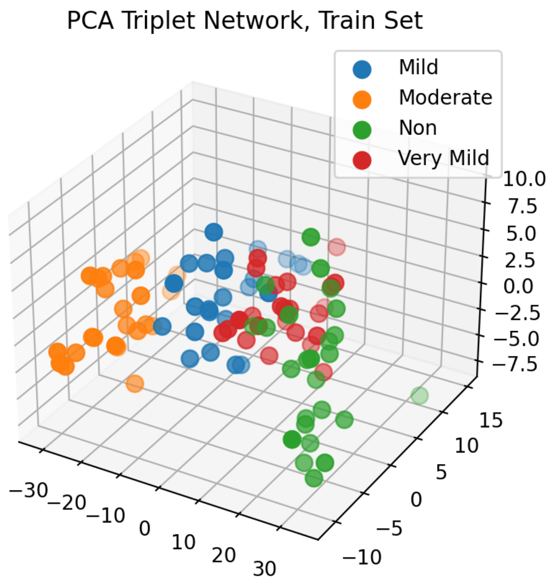

(a)

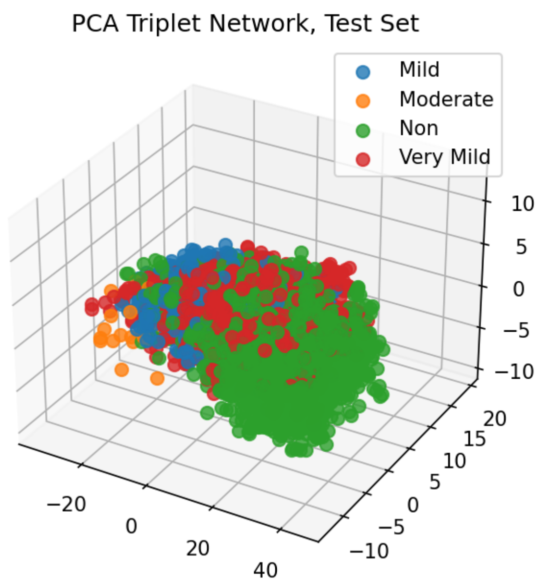

(b)

Figure 5.9: Triplet Network Embeds, “From Scratch” Model, 3-dimensions

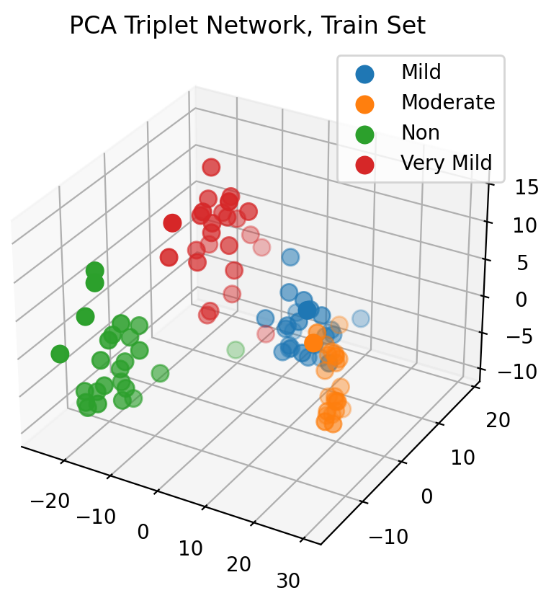

(a)

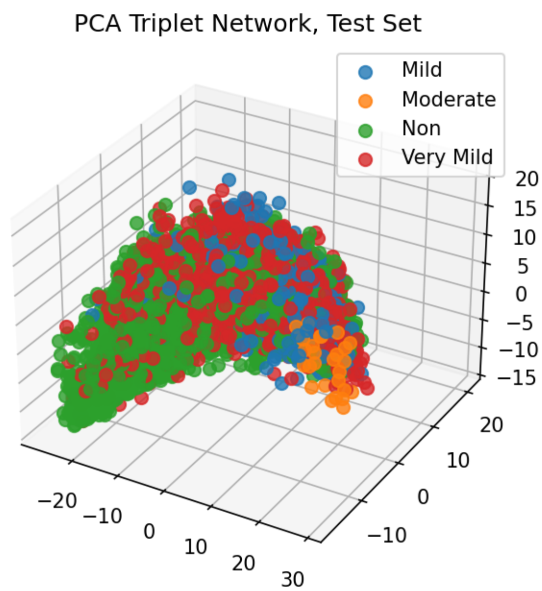

(b)

Figure 5.10: Triplet Network Embeds, Transfer Model, 3-dimensions

5.6 Results and Discussion

All of the models were able to separate the training samples well. As reflected by the accuracy and PCA visualizations, the test set isn't as well separated, but still has some structure. This is partly due to the training set not having samples from all slice depths. The structure of the brain varies drastically based on depth of the slice taken. From our experiments the models are not able to generalize well to slice depths it has not seen, we will discuss this more in the next chapter when we discuss limitations.

For the Siamese models, they learned very different ways to separate the classes. For the "From Scratch" model, it appears to have learned the relation of each class to the others. In other words, non demented cases are closest to very mild, very mild is in between non demented and mild, mild is between very mild and moderate, and moderate is only closest to mild. In the case of the transfer learned model, it was not able to learn this relation. This likely due to the combination of using a pretrained model, i.e. one that is in a "good" state, and contrastive loss. For the Triplet networks, both training methods were able to learn the relation between each stage of the disease, although slightly different. The transfer learned model differed from that of the Siamese one due to the triplet loss. Rather than only be able to 'push' two points away if they were different, or 'pull' them together if they similar, the triplet loss could do both at the same time. This effect has been seen before in other medical imaging domains [4, 16]. However, our results are obtained via PCA rather than t-SNE, a different dimensionality reduction technique.

Based on our results, a transfer learned Siamese network might not be as useful compared to the other three. The other three models benefit from the fact that when querying the trained model if a sample embedding is in between two classes it could be assumed that the input belongs to one of the classes. The transfer learned Siamese model does not have this benefit, since the embeds do not appear to follow a progression like the other three.

Chapter 6

Limitations and Future Work

6.1 Limitations

The most impactful limitation for both of our methods is the lack of knowledge of the collection process of the dataset. There are numerous types of MRI scans that can be done on the brain such as T1-weighted and T2-weighted; the images in the dataset we use appear to be T1-weighted since the white matter is lighter in color than the gray matter. Another issue is no indication of what range of slices that the MRI sequences came from, as well as how many unique brains there are; typically, when a patient gets an MRI done multiple slices of the brain are taken. Take for example, the images in Figure 6.1, both brains are non-demented, but their structure is very different because they are from different depths. This proved to be an issue at the start of our research. The supplied training set contained few examples of the ventricular sections of the brain for all classes. While the supplied testing set consisted mostly of the ventricular sections. This caused lower than expected accuracy for our ResNet-18 model in initial test runs. To counter this, we merged the given sets and performed our own randomized split, resulting in higher accuracy. This problem is still evident with the results of the Siamese and Triplet networks.

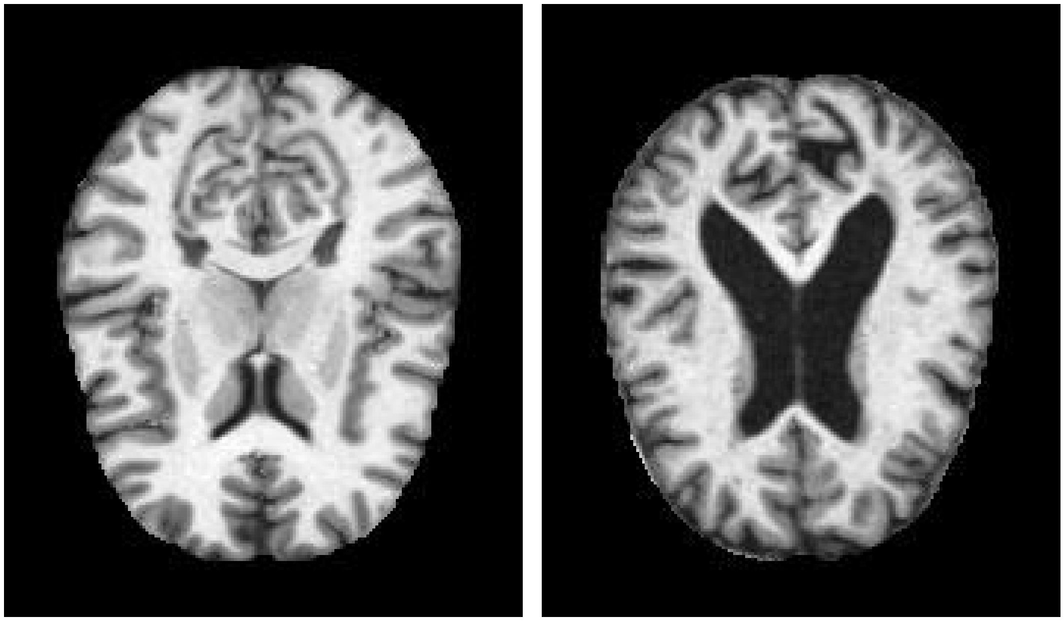

Figure 6.1: Different Brain Slices

6.2 Future Work

While our method for visualizing features was applied to ResNet-18, future work might explore using different models. Different model architectures learn differently, being able to visually explain the network helps validate the model. Future work might also deal with having results validated with a clinical professional.

Future work on Siamese and Triplet networks might explore:

- Treating a patient's entire MRI scan sequence, i.e. all the slices, as 'one' sample, rather than just a single slice.
- Use each sample is a slice at a different depth, instead of random selection.
- Pretrain the network from a different brain imagery task.
- Use volumetric 3D MRI scans

Having the data sampling be patient based rather than image based might be more logical as MRI scans typically contain a sequence of slices rather than a single slice. This has the added benefit of more raw data to train with, most likely improving performance. For the second, having the model train on at least one sample per depth allows the model to 'see' an example of the brain at every depth. For the third, Siamese and Triplet networks are typically pretrained on a similar but disjoint task; pretraining the model from a different brain imagery task might help to improve performance. Finally, using a 3D volumetric MRI scan of the brain allows the model to learn from the entire brain rather than segments at a time.

Chapter 7

Conclusions

Deep learning has become a standard approach for medical imaging tasks; however, deep learning has its caveats. We had two goals for this thesis. First, aide in explaining deep learning models. Second, train a network on limited amounts of data. For the first, we trained a conventional network on an adequate amount of data and used two different visualization techniques: saliency maps, which are commonly used, and a "deep dream" style feature extraction, which has not been used, to our knowledge, in medical imaging. For the second, we used two metric learning models that train on limited amounts of data. By training on limited amounts of data we reduce the requirement of large amounts of data that needs to be collected, which can be costly. Both of these methods are important steps to help increase the adoption of deep learning in the medical sector.

Bibliography

[1] 2021 alzheimer's disease facts and figures. *Alzheimer's & Dementia*, 17(3):327–406, 2021.

[2] Tooba Altaf, Syed Muhammad Anwar, Nadia Gul, Muhammad Nadeem Majeed, and Muhammad Majid. Multi-class alzheimer's disease classification using image and clinical features. *Biomedical Signal Processing and Control*, 43:64–74, May 2018.

[3] Jane Bromley, Isabelle Guyon, Yann LeCun, Eduard Säckinger, and Roopak Shah. Signature verification using a "siamese" time delay neural network. In *Advances in Neural Information Processing Systems*, volume 6. Morgan-Kaufmann, 1994.

[4] Yu-An Chung and Wei-Hung Weng. Learning deep representations of medical images using siamese cnns with application to content-based image retrieval. *arXiv:1711.08490 [cs]*, Dec 2017. arXiv: 1711.08490.

[5] Jia Deng, Wei Dong, Richard Socher, Li-Jia Li, Kai Li, and Li Fei-Fei. Imagenet: A large-scale hierarchical image database. In *2009 IEEE conference on computer vision and pattern recognition*, pages 248–255. Ieee, 2009.

[6] Fabian Eitel and Kerstin Ritter. Testing the robustness of attribution methods for convolutional neural networks in mri-based alzheimer's disease classification. *arXiv:1909.08856 [cs, eess]*, Sep 2019. arXiv: 1909.08856.

[7] Kunihiko Fukushima. Neocognitron: A self-organizing neural network model for a mechanism of pattern recognition unaffected by shift in position. *Biological Cybernetics*, 36(4):193–202, Apr 1980.

[8] Lawrence V. Fulton, Diane Dolezel, Jordan Harrop, Yan Yan, and Christopher P. Fulton. Classification of alzheimer's disease with and without imagery using gradient boosted machines and resnet-50. *Brain Sciences*, 9(9):212, Aug 2019.

[9] R. Hadsell, S. Chopra, and Y. LeCun. Dimensionality reduction by learning an invariant mapping. In *2006 IEEE Computer Society Conference on Computer Vision and Pattern Recognition - Volume 2 (CVPR'06)*, volume 2, page 1735–1742. IEEE, 2006.

[10] Kaiming He, Xiangyu Zhang, Shaoqing Ren, and Jian Sun. Deep residual learning for image recognition. In *2016 IEEE Conference on Computer Vision and Pattern Recognition (CVPR)*, page 770–778, Jun 2016.

[11] Elad Hoffer and Nir Ailon. Deep metric learning using triplet network. In Aasa Feragen, Marcello Pelillo, and Marco Loog, editors, *Similarity-Based Pattern Recognition*, pages 84–92, Cham, 2015. Springer International Publishing.

[12] G. B. Karas, P. Scheltens, S. A. R. B. Rombouts, P. J. Visser, R. A. van Schijndel, N. C. Fox, and F. Barkhof. Global and local gray matter loss in mild cognitive impairment and alzheimer's disease. *NeuroImage*, 23(2):708–716, Oct 2004.

[13] Gregory Koch, Richard Zemel, and Ruslan Salakhutdinov. Siamese neural networks for one-shot image recognition. *International Conference on Machine Learning*, 2015.

[14] Salim Lahmiri and Mounir Boukadoum. Alzheimer's disease detection in brain magnetic resonance images using multiscale fractal analysis. *ISRN Radiology*, 2013, Oct 2013.

[15] Salim Lahmiri and Mounir Boukadoum. New approach for automatic classification of alzheimer's disease, mild cognitive impairment and healthy brain magnetic resonance images. *Healthcare Technology Letters*, 1(1):32–36, Jun 2014.

[16] Chin-Fu Liu, Shreyas Padhy, Sandhya Ramachandran, Victor X. Wang, Andrew Efimov, Alonso Bernal, Linyuan Shi, Marc Vaillant, J. Tilak Ratnanather, Andreia V. Faria, and et al. Using deep siamese neural networks for detection of brain asymmetries associated with alzheimer's disease and mild cognitive impairment. *Magnetic resonance imaging*, 64:190–199, Dec 2019.

[17] Abhishaike Mahajan, James Dormer, Qinmei Li, Deji Chen, Zhenfeng Zhang, and Baowei Fei. Siamese neural networks for the classification of high-dimensional radiomic features. *Proceedings of SPIE–the International Society for Optical Engineering*, 11314:113143Q, Feb 2020.

[18] Alexander Mordvintsev, Christopher Olah, and Mike Tyka. Inceptionism: Going deeper into neural networks, 2015.

[19] Anh Nguyen, Jason Yosinski, and Jeff Clune. Deep neural networks are easily fooled: High confidence predictions for unrecognizable images. *arXiv:1412.1897 [cs]*, Apr 2015. arXiv: 1412.1897.

[20] Anh Nguyen, Jason Yosinski, and Jeff Clune. Multifaceted feature visualization: Uncovering the different types of features learned by each neuron in deep neural networks. Feb 2016.

[21] Kanghan Oh, Young-Chul Chung, Ko Woon Kim, Woo-Sung Kim, and Il-Seok Oh. Classification and visualization of alzheimer's disease using volumetric convolutional neural network and transfer learning. *Scientific Reports*, 9(1):18150, Dec 2019.

[22] Chris Olah, Alexander Mordvintsev, and Ludwig Schubert. Feature visualization. *Distill*, 2017. https://distill.pub/2017/feature-visualization.

[23] Adam Paszke, Sam Gross, Francisco Massa, Adam Lerer, James Bradbury, Gregory Chanan, Trevor Killeen, Zeming Lin, Natalia Gimelshein, Luca Antiga, Alban Desmaison, Andreas Kopf, Edward Yang, Zachary DeVito, Martin Raison, Alykhan Tejani, Sasank Chilamkurthy, Benoit Steiner, Lu Fang, Junjie Bai, and Soumith Chintala. Pytorch: An imperative style, high-performance deep learning library. In *Advances in Neural Information Processing Systems 32*, pages 8024–8035. Curran Associates, Inc., 2019.

[24] Kenneth A. Philbrick, Kotaro Yoshida, Dai Inoue, Zeynettin Akkus, Timothy L. Kline, Alexander D. Weston, Panagiotis Korfiatis, Naoki Takahashi, and Bradley J. Erickson. What does deep learning see? insights from a classifier trained to predict contrast enhancement phase from ct images. *American Journal of Roentgenology*, 211(6):1184–1193, Dec 2018.

[25] Maithra Raghu, Chiyuan Zhang, Jon Kleinberg, and Samy Bengio. Transfusion: Understanding transfer learning for medical imaging. In *Advances in Neural Information Processing Systems*, volume 32. Curran Associates, Inc., 2019.

[26] Farheen Ramzan, Muhammad Usman Ghani Khan, Asim Rehmat, Sajid Iqbal, Tanzila Saba, Amjad Rehman, and Zahid Mehmood. A deep learning approach for automated diagnosis and multi-class classification of alzheimer's disease stages using resting-state fmri and residual neural networks. *Journal of Medical Systems*, 44(2):37, Dec 2019.

[27] Johannes Rieke, Fabian Eitel, Martin Weygandt, John-Dylan Haynes, and Kerstin Ritter. Visualizing convolutional networks for mri-based diagnosis of alzheimer's disease. *arXiv:1808.02874 [cs]*, 11038:24–31, 2018. arXiv: 1808.02874.

[28] D Salas-Gonzalez, J M Górriz, J Ramírez, M López, I Álvarez, F Segovia, R Chaves, and C G Puntonet. Computer-aided diagnosis of alzheimer's disease using support vector machines and classification trees. *Physics in Medicine & Biology*, 55(10):2807–2817, apr 2010.

[29] Mohammad Shorfuzzaman and M. Shamim Hossain. Metacovid: A siamese neural network framework with contrastive loss for n-shot diagnosis of covid-19 patients. *Pattern Recognition*, 113:107700, May 2021.

[30] Karen Simonyan, Andrea Vedaldi, and Andrew Zisserman. Deep inside convolutional networks: Visualising image classification models and saliency maps. *arXiv:1312.6034 [cs]*, Apr 2014. arXiv: 1312.6034.

[31] Haijing Sun, Anna Wang, Wenhui Wang, and Chen Liu. An improved deep residual network prediction model for the early diagnosis of alzheimer's disease. *Sensors (Basel, Switzerland)*, 21(12):4182, Jun 2021.

[32] Jason Yosinski, Jeff Clune, Yoshua Bengio, and Hod Lipson. How transferable are features in deep neural networks? In *Advances in Neural Information Processing Systems*, volume 27. Curran Associates, Inc., 2014.